

Diffraction in the Semiclassical Approximation to Feynman's Path Integral Representation of the Green Function

Martin Schaden and Larry Spruch
New York University, Physics Department
4 Washington Place, New York, New York 10003

October 30, 2018

Abstract

We derive the semiclassical approximation to Feynman's path integral representation of the energy Green function of a massless particle in the shadow region of an ideal obstacle in a medium. The wavelength of the particle is assumed to be comparable to or smaller than any relevant length of the problem. Classical paths with extremal length partially creep along the obstacle and their fluctuations are subject to non-holonomic constraints. If the medium is a vacuum, the asymptotic contribution from a single classical path of overall length L to the energy Green function at energy E is that of a non-relativistic particle of mass E/c^2 moving in the two-dimensional space orthogonal to the classical path for a time $\tau = L/c$. Dirichlet boundary conditions at the surface of the obstacle constrain the motion of the particle to the exterior half-space and result in an effective time-dependent but spatially constant force that is inversely proportional to the radius of curvature of the classical path. We relate the diffractive, classically forbidden motion in the "creeping" case to the classically allowed motion in the "whispering gallery" case by analytic continuation in the curvature of the classical path. The non-holonomic constraint implies that the surface of the obstacle becomes a zero-dimensional caustic of the particle's motion. We solve this problem for extremal rays with piecewise constant curvature and provide uniform asymptotic expressions that are approximately valid in the penumbra as well as in the deep shadow of a sphere.

PACS: 03.65.Sq, 42.25.Fx, 11.15.Kc

1 Introduction

It was some three hundred years after Descartes's work on diffraction theory that Keller[1] provided a sound mathematical foundation for the theory by examining

the asymptotic expansion of the energy Green function. Armed with that solid footing, and using considerable physical insight, Keller and co-workers[2, 3] and others[4] found a host of applications. Though the theory has had any number of successes, its application can sometimes be cumbersome and its validity is limited to the deep-shadow region. The limitation is not really a restriction in the asymptotic evaluation for high energies, since any point in this case is either in the lit or the deep shadow region of an obstacle. It does however point to the limitations of the approach itself that have only been overcome[5, 6] by considering a different expansion in the penumbra.

All these approaches are purely classical, based on the eikonal- (or ray-) approximation to the wave equation. The asymptotic forms of the wave function and of the energy Green function thereby obtained give the diffraction pattern for wave number $k \sim \infty$, providing the leading correction to geometrical optics due to diffraction. Keller interpreted his result[1] geometrically in terms of paths, including those of certain "creeping" rays, a very physical and useful way of viewing the problem. We here study diffraction from the point of view of a semiclassical expansion. Our starting point is the Feynman path integral representation for the Green function of a massless scalar field in the presence of ideal obstacles. To simplify the presentation we assume Dirichlet boundary conditions for the field at the surface of the obstacles and often assume a uniform surrounding medium. We analyze and approximate the path integral representation of the Green function semiclassically. Note that Feynman's approach was published in 1949[7], but its advantages for obtaining asymptotic solutions – not only technically, but in the clearer physical picture it provides – may not have been apparent at the time the modern version of diffraction theory was developed. Furthermore, it seemed natural to attack a classical theory classically. In fact, Gutzwiller[8] and others have made significant advances in the semiclassical evaluation of the path integral. To our knowledge these advantages of Feynman's formulation and Gutzwiller's semiclassical evaluation have never been fully exploited in the case of diffraction theory. (Some related approaches by others will be briefly commented on below.) We here hope to help close this gap.

That an asymptotic analysis of the classical wave equation for large k should give the same result as the semiclassical expansion is well known but may nevertheless warrant a remark. For simplicity, we assume for the moment that the medium is uniform. Since the connection between the local wave number k and the energy E of a massless particle is

$$k = E/(\hbar v(E)) , \tag{1}$$

where $v(E)$ is the phase velocity in the medium, letting k be arbitrarily large is equivalent to letting \hbar be arbitrarily small.

Our final result is equivalent to those obtained previously in certain limits. However, the present development may have a number of conceptual advantages. The illuminated region, the penumbra and the umbra are all treated in a unified fashion. The approach furthermore is probably more accessible to most

physicists than the original one, and might provide new insights. By providing a different point of view of the phenomenon, it may also suggest other (interpolating) approximations. Perhaps the most interesting aspect of the present formulation is that it provides a systematic geometrical framework that in principle allows one to obtain asymptotic expressions for diffraction for many systems, although considerable numerical work may be necessary if the geometrical setting is sufficiently complicated; in particular, it shows that diffraction can be understood as a special case of quantum mechanical tunnelling in the sense that the corresponding motion is classically forbidden and that the semiclassical approximation is obtained by analytic continuation in some of the parameters of the problem.

We will study the semiclassical approximation, $G(\mathbf{Y}, \mathbf{X}; E)$, to the energy Green function

$$G(\mathbf{X}, \mathbf{Y}; E) \equiv \langle \mathbf{Y} | \hat{\mathcal{G}}(E + i\eta) | \mathbf{X} \rangle = \langle \mathbf{Y} | (\hat{H} - E - i\eta)^{-1} | \mathbf{X} \rangle, \quad (2)$$

the coordinate representation of the Laplace transform of the time evolution operator. For simplicity we will study only the propagation of a free massless scalar particle in a medium which, for the most part, will be taken to be homogeneous. We require that \mathcal{G} vanish for $|\mathbf{X} - \mathbf{Y}| \rightarrow \infty$ and also whenever \mathbf{X} or \mathbf{Y} are on a smooth compact (but not necessarily connected) two-dimensional surface \mathcal{F} . These Dirichlet boundary conditions are also the appropriate ones for a particular polarization of the electromagnetic field in the presence of ideal conductors. Note that semiclassically only photons whose polarization is normal to the surface can diffract in the case of an ideal conductor.

Green functions are among the most basic concepts in physics. Thus, for example, the trace of $\hat{\mathcal{G}}(E + i\eta)$ is the response function $g(E)$, whose imaginary part gives the spectral density $\rho(E)$, where $\rho(E)dE$ is the number of states with energy between E and $E + dE$. Unfortunately, Green functions can rarely be obtained exactly. An exceedingly useful result, largely due to Gutzwiller[8], is the observation that the semi-classical approximation to $\mathcal{G}(\mathbf{Y}, \mathbf{X}; E)$ and $g(E)$ are usually completely determined by the solution of a corresponding *classical* problem. Unfortunately, the solution must be modified if it is to be used in the case of diffraction. The corresponding classical trajectories are *non-holonomic* constrained extrema of the action that are not stationary; the dependence of the action on the fluctuations therefore contains linear terms. A naive application of the usual semiclassical approximation fails. We will see that the semiclassical Green function $G(\mathbf{Y}, \mathbf{X}; E)$ nevertheless *is* given by the solution to a corresponding classical problem in this case too. The corresponding classical problem one has to solve in the case of diffraction is that of the motion of a non-relativistic particle in two dimensions under the influence of a generally time-dependent gravitational-like acceleration inversely proportional to $R(s(t))$ in the presence of a ceiling; $R(s(t))$ is the radius of curvature of the constrained *classical* trajectory connecting \mathbf{X} and \mathbf{Y} as a function of the arc length $s(t)$.

Our interest in semiclassical diffraction theory was rekindled in the course of a study of Casimir effects. We found that a semiclassical evaluation gives

the leading behavior whenever the Casimir energy diverges [9] as one length scale of the problem is taken to be much larger than any other. In many cases this asymptotic evaluation is sufficient to determine the Casimir energy *exactly*. A phenomenologically interesting example is Derijaguin’s problem[10] of the Casimir force between two conducting spheres of radii R_1 and R_2 in the limit where their separation d is arbitrarily small compared to R_1 and R_2 . This force had been determined using very plausible arguments[10, 11], but the semiclassical calculation provided what we believe to be the first rigorous derivation of this result. The Casimir force in this limiting case is proportional to \bar{R}/d^3 , where $\bar{R} = R_1 R_2 / (R_1 + R_2)$, and diverges as $\bar{R}/d \rightarrow \infty$; the semiclassical calculation gives the correct coefficient. On the other hand, for separations large compared with the radius of either sphere, the Casimir-Polder force[12] falls off as $1/d^8$ and *a priori* one cannot assert that the semiclassical approximation must be exact in this case. To see whether this approximation qualitatively reproduces the $1/d^8$ behavior of the force in this limit, one has to take diffraction into account at least semiclassically. The effort to include these effects and thus perhaps extend the validity of the semiclassical calculation beyond the regime $d \ll \bar{R}$ led us to the present study. The extension to $d \gtrsim \bar{R}$ is under consideration.

In Sec. II we present a heuristic argument based on Fermat’s principle to derive the effective action for the semiclassical approximation to the path-integral representation of the energy Green function of a massless particle in the presence of idealized obstacles. There is no stationary classical path that can describe propagation into the shadow region of the obstacle. The situation turns out to be analogous to that of calculating the amplitude that a non-relativistic particle move in finite time from the ceiling to the ceiling under the influence of a gravitational force. We show in Sec. III that an analytic continuation in the parameters solves the problem by changing it to that of a non-relativistic particle moving in finite time from the floor to the floor under the influence of a gravitational-like force – the same problem encountered in the semiclassical description of ”whispering galleries”. The remainder of Sec. III is devoted to an analytical study of diffraction by a sphere. In Sec. IV we relate the description by classical trajectories in a gravitational-like field to Keller’s asymptotic evaluation of the energy Green function for this example. In particular, we also derive the power corrections of the asymptotic expansion within this unified approach.

There is an immense literature on the subject. See, for example Gutzwiller[8] and Reichl[13], and references therein. We also include a small sampling of recent developments on caustics[14].

2 The Action: A Heuristic Argument

Our ultimate goal is to obtain the semiclassical approximation $G(\mathbf{X}, \mathbf{Y}; E)$ to $\mathcal{G}(\mathbf{X}, \mathbf{Y}; E)$, the probability amplitude that a photon of energy E at the initial point \mathbf{X} will at some time appear at \mathbf{Y} . Since the semiclassical energy Green function is essentially determined by the quadratic action S^{sc} for the fluctu-

ations – as we will discuss later – we first determine the form of this action. (See Eq. (17) below.)

2.1 The Action for the Fluctuations to Quadratic Order

We argue that the contribution to the energy Green function of a continuous path γ from \mathbf{X} to \mathbf{Y} is determined by the action

$$S(\gamma, E) = E\tau(\gamma, E) = E \int_0^T dt |\dot{\mathbf{X}}(t)|/v(\mathbf{X}(t), E). \quad (3)$$

A path γ from \mathbf{X} to \mathbf{Y} in this context is defined by the three continuous functions on the interval $0 \leq t \leq T$ that make up the vector $\mathbf{X}(t)$ and satisfy $\mathbf{X}(0) = \mathbf{X}$ and $\mathbf{X}(T) = \mathbf{Y}$. The variable $t \in [0, T]$ need not be the actual time, since the integral in Eq. (3) does not depend on how the path is parameterized. Using the arc length s along the path γ , one may rewrite $S(\gamma, E)$ as

$$S(\gamma, E) = E \int_0^{L_\gamma} \frac{ds}{v(s, E)}, \quad (4)$$

where L_γ is the path's total length. For the semiclassical quantization it will be important that Eq. (3) in fact does not depend on the "speed" $|\dot{\mathbf{X}}|$, subject to the restriction that $|\dot{\mathbf{X}}|$ never vanish along the path (or equivalently that the arc length is a monotonically increasing function of the parameter t). $2\pi\nu\tau(\gamma, E)$ is the phase lag of a monochromatic wave of frequency $\nu = E/(2\pi\hbar)$ along the path γ with the phase velocity $v(s, E)$ related to the *local* index of refraction $n(s, \nu) = c/v(s, E)$ of the medium along the path. Fermat's principle is the statement that the "classical" trajectory γ_c of a monochromatic ray is an extremum of τ . It is the phase velocity that determines the *trajectory* of a monochromatic ray (as is for instance evident from Snell's law). Other than when the medium is a vacuum, the time $\tau(\gamma_c, E)$ is *not* the time between emission at \mathbf{X} and absorption at \mathbf{Y} of a *photon* of frequency ν . The travel time for a photon or, classically, a wave-packet, is determined by the local group velocity $v_g(s, E)$ along the path,

$$v_g^{-1}(s, E) = \frac{\partial}{\partial E} \left(\frac{E}{v(s, E)} \right), \quad (5)$$

that is, the time \mathcal{T} for a photon of energy E to travel from \mathbf{X} to \mathbf{Y} is

$$\mathcal{T} = \int_0^{L_\gamma} \frac{ds}{v_g(s, E)} = \frac{\partial}{\partial E} \int_0^{L_\gamma} ds \frac{E}{v(s, E)} = \frac{\partial S(\gamma, E)}{\partial E}. \quad (6)$$

The relation Eq. (6) between the total time \mathcal{T} and the quantity S defined by Eq. (3), in conjunction with Fermat's principle, identifies $S(\gamma, E)$ as the classical action that describes the motion of a massless particle (uniquely up to an irrelevant constant that does not depend on the energy nor on the path γ).

Hamilton's principal function $R(\mathbf{X}, \mathbf{Y}; \mathcal{T})$ with the independent variable \mathcal{T} is the Legendre transform of S ,

$$R(\mathbf{X}, \mathbf{Y}; \mathcal{T}) = S(\mathbf{X}, \mathbf{Y}, E) - E\mathcal{T} = E^2 \frac{\partial}{\partial E} \int_0^{L_\gamma} \frac{ds}{v(s, E)} \Big|_{E \rightarrow E(\mathcal{T})} \quad (7)$$

and vanishes in a vacuum, as it must, because the Minkowski distance between the events vanishes and Hamilton's principal function is proportional to it.

We temporarily restrict our considerations to the situation where the phase velocity $v(\mathbf{X}(t), E) = v(E)$ is constant when $\mathbf{X}(t)$ is exterior to the volume \mathcal{V} with surface \mathcal{F} and vanishes when $\mathbf{X}(t)$ is in the interior of \mathcal{V} . This is an idealized limit of the physical situation where obstacles with a very high index of refraction are embedded in a homogeneous medium. The index of refraction in the physical case depends smoothly on the coordinates and the classical paths are stationary points of the action. The action defined by Eq. (3) of a path that avoids \mathcal{V} in going from \mathbf{X} to \mathbf{Y} is proportional to its length. The vanishing phase velocity in the interior of \mathcal{V} leads to a non-holonomic constraint on the classical motion. We will see that the situation is akin to motion in a gravitational-like potential in the presence of a ceiling. The classical motion is still an extremum of the action, simply because the constraint can be viewed as a particular *limit* of the physical case. In the limit, the extremum generally is not a stationary point of the action. The change of the action under some small deviations from the extreme path can no longer be made arbitrarily small in this limit, that is, the functional derivative of the action at the extremum does not exist.

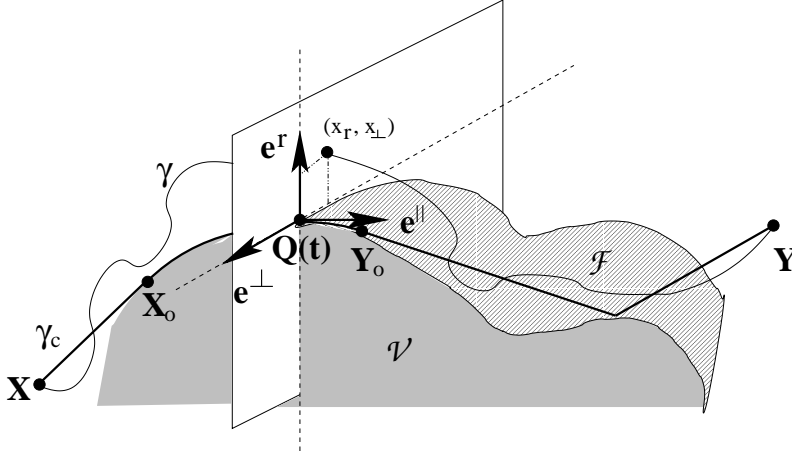


Fig. 1: The semiclassical expansion. The bold curve is a schematic plot of a classical path γ_c of extremal length from \mathbf{X} to \mathbf{Y} that is excluded from the (smooth) volume \mathcal{V} . The length of γ_c is extremal but not stationary, since it "creeps" along the surface between the points \mathbf{X}_o and \mathbf{Y}_o . A non-extremal path γ in the vicinity of this classical path is shown as a thin line and the local coordinate frame at the point $\mathbf{Q}(t)$ of γ_c is sketched. The fluctuation γ is fully described by the coordinates $x_r(t)$ and $x_\perp(t)$ of local coordinate frames along the whole classical path. Note that \mathbf{e}^\perp lies in the surface \mathcal{F} .

As can be seen from Fig.1, the classical trajectory of extremal length from \mathbf{X} to \mathbf{Y} can be rather complicated even in the presence of smooth obstacles. It may consist not only of straight sections and reflections off points on the surface, but also of segments that “creep” along the surface. The classical trajectory is by definition continuous and of extremal length in coordinate space. It is natural to parameterize it by the “intrinsic” time t for which $s(t) = v(E)t$ is the arc length along the classical path. In this case the instantaneous velocity $\dot{\mathbf{X}}_c(t)$ and the instantaneous acceleration $\ddot{\mathbf{X}}_c(t)$ are orthogonal vectors, since $|\dot{\mathbf{X}}_c(t)| = v(E)$ does not depend on time.

This singles out a natural local orthonormal coordinate frame at each point along curved sections of the classical path. The basis vectors of this local coordinate frame are

$$\mathbf{e}^{\parallel}(t) = \frac{\dot{\mathbf{X}}(t)}{v(E)}, \quad \mathbf{e}^r(t) = -\frac{R(t)}{v^2(E)}\ddot{\mathbf{X}}(t), \quad \mathbf{e}^{\perp}(t) = \mathbf{e}^{\parallel}(t) \times \mathbf{e}^r(t), \quad (8)$$

where the local radius of curvature of the classical path is related to the instantaneous acceleration by $R(t) = v^2(E)/|\ddot{\mathbf{X}}(t)|$. $\mathbf{e}^{\parallel}(t)$ clearly is parallel to the velocity $\dot{\mathbf{X}}(t)$ and thus tangent to the classical path, $\mathbf{e}^r(t)$ lies in the local plane of motion (and is normal to the surface of the obstacle) while $\mathbf{e}^{\perp}(t)$ is perpendicular to the local plane (and lies in the surface of the obstacle). On straight sections of the classical path a similar local orthonormal coordinate frame exists, but is not uniquely defined with respect to rotations about the classical path.

We next introduce local coordinates that give the deviation of the path γ from a classical path γ_c that is an extremum of the action in Eq. (3). Let $\mathbf{X}_c(t)$ and $\mathbf{X}(t)$ describe a point on the classical trajectory γ_c and a point on the path γ in a (time-independent) global coordinate frame at the intrinsic time t of the classical path. The coordinates $x_{\parallel}(t)$, $x_r(t)$ and $x_{\perp}(t)$ for the fluctuations in the local basis at time t are then defined by

$$\mathbf{X}(t) = \mathbf{X}_c(t) + x_{\parallel}(t)\mathbf{e}^{\parallel}(t) + x_r(t)\mathbf{e}^r(t) + x_{\perp}(t)\mathbf{e}^{\perp}(t). \quad (9)$$

where $\mathbf{X}(t)$ is a point on γ . (See Fig. 1). It is important to note that certain fluctuations just reparameterize the classical path. This follows from our earlier observation that the speed along the path plays no role. More formally, if instead of the intrinsic time t one had chosen t' , where

$$t' = t + \eta(t), \quad (10)$$

to parameterize the classical path, then to first order in $\eta(t)$

$$\mathbf{X}_c(t') = \mathbf{X}_c(t) + \eta(t)\dot{\mathbf{X}}_c(t) + \dots = \mathbf{X}_c(t) + \eta(t)v(E)\mathbf{e}^{\parallel}(t) + \dots \quad (11)$$

An infinitesimal longitudinal fluctuation, $x_{\parallel}(t) = \eta(t)v(E)$, thus describes the *same* classical path and is equivalent to the use of a slightly different “clock”

to parameterize the classical path. To avoid this ambiguity and have a one-to-one correspondence between the fluctuations and paths, one considers only fluctuations in the planes

$$x_{\parallel}(t) = 0 . \quad (12)$$

We can do so, because the local coordinates $x_r(t)$ and $x_{\perp}(t)$ in each plane along the classical path γ_c completely specify γ . The geometrical meaning and uniqueness of this construction can be seen in Fig. 1.

We will also need to know how the basis vectors defined by Eq. (8) rotate with time. Since, by Eq. (8),

$$\dot{\mathbf{e}}^{\parallel}(t) = \ddot{\mathbf{X}}(t)/v(E) = -v(E)\mathbf{e}^r(t)/R(t) \quad (13)$$

is in the direction of one of the basis vectors, the rotation of the coordinate frame with time is specified by only two (generally time-dependent) angular velocities, instead of the usual three. The basis at time t is related to the basis at time $t + dt$ by an infinitesimal orthogonal transformation Ω . $\mathbf{e}^{\parallel}(t + dt)$ thus is given in terms of the elements of Ω and of the $\mathbf{e}(t)$'s of Eq. (8). Comparing the resulting expression with Eq. (13) determines two of the three independent elements of Ω . Denoting the as yet to be determined independent element of Ω by $\alpha(t)$, one obtains

$$\dot{\mathbf{e}}^{\parallel}(t) = -\frac{v(E)}{R(t)}\mathbf{e}^r(t), \quad \dot{\mathbf{e}}^r(t) = \frac{v(E)}{R(t)}\mathbf{e}^{\parallel}(t) - \alpha(t)\mathbf{e}^{\perp}(t), \quad \dot{\mathbf{e}}^{\perp}(t) = \alpha(t)\mathbf{e}^r(t). \quad (14)$$

Explicitly differentiating $\mathbf{e}^r(t)$ in Eq. (8) and taking the inner product with $\mathbf{e}^{\perp}(t)$ determines $\alpha(t)$ as

$$\alpha(t) = \frac{R(t)}{v^2(E)}(\ddot{\mathbf{X}}_c(t) \cdot \mathbf{e}^{\perp}(t)). \quad (15)$$

$\alpha(t)$ vanishes if the classical trajectory lies in a plane and thus is a measure of its skewness. It is the rate at which the coordinate frame rotates about the tangent vector to the classical path. For a helix on a cylinder of radius R_{cyl} , a velocity v_z parallel to the cylinder axis and an angular velocity ω , one finds $\alpha(t) = -\omega v_z / \sqrt{v_z^2 + (\omega R_{\text{cyl}})^2}$, independent of time[15].

We are now in a position to expand the action of Eq. (3) to quadratic order in the fluctuations $x_{\parallel} = 0, x_r(t), x_{\perp}(t)$ that uniquely describe a path in the vicinity of the classical one. Taking the time derivative of Eq. (9) and using Eq. (14) to describe the time dependence of the basis one finds

$$\begin{aligned} \dot{\mathbf{X}}(t) = & [(\dot{x}_r(t) + \alpha(t)x_{\perp}(t))\mathbf{e}^r(t) + (\dot{x}_{\perp}(t) - \alpha(t)x_r(t))\mathbf{e}^{\perp}(t)] \\ & + v(E) \left(1 + \frac{x_r(t)}{R(t)}\right) \mathbf{e}^{\parallel}(t). \end{aligned} \quad (16)$$

As noted earlier $v(E)\mathbf{e}^{\parallel}(t)$ is the velocity $\dot{\mathbf{X}}_c(t)$ along the classical trajectory. [Eq. (8) gives the same relationship, but with $\mathbf{X}_c(t)$ rather than $\mathbf{X}(t)$. There

is no inconsistency, since we have chosen $x_{\parallel}(t) = 0$.] Expanding the action of Eq. (3) to quadratic order in the fluctuations using Eq. (16), one finally obtains

$$S_{\gamma_c}^{sc}(\gamma, E) = \int_0^{\tau(\gamma_c, E)} dt \left\{ E + E \frac{x_r(t)}{R(t)} + \frac{E}{2v^2(E)} \left[(\dot{x}_r(t) + \alpha(t)x_{\perp}(t))^2 + (\dot{x}_{\perp}(t) - \alpha(t)x_r(t))^2 \right] \right\} \quad (17)$$

for the action of the path γ in semiclassical approximation, when the classical path is γ_c . Note that the term *linear* in the fluctuations of the semiclassical action (17) is due to the fact that the classical path, constrained to lie outside of \mathcal{V} , is extremal, but not stationary. Since the classical trajectory described by $x_r(t) = x_{\perp}(t) = 0$ creeps along the surface \mathcal{F} whenever $0 < R(t) < \infty$ and since $\mathbf{e}^r(t)$ is normal to \mathcal{F} at that point, the coordinate $x_r(t)$ takes only positive values on a creeping segment. The kinetic terms in Eq. (17) are those of a non-relativistic particle of mass

$$m_E = E/v^2(E) \quad (18)$$

moving in a plane that is rotating with angular velocity $\alpha(t)$. To explicitly see this, we perform a time-dependent orthogonal transformation of the coordinates

$$\begin{aligned} x_r(t) &= \underline{x}_r(t) \cos \theta(t) - \underline{x}_{\perp}(t) \sin \theta(t) \\ x_{\perp}(t) &= \underline{x}_r(t) \sin \theta(t) + \underline{x}_{\perp}(t) \cos \theta(t) \end{aligned} \quad (19)$$

with

$$\theta(t) = \int_0^t dt' \alpha(t'). \quad (20)$$

The expressions in Eq. (17) are then

$$\begin{aligned} \dot{x}_r(t) + \alpha(t)x_{\perp}(t) &= \dot{\underline{x}}_r(t) \cos \theta(t) - \dot{\underline{x}}_{\perp}(t) \sin \theta(t) \\ \dot{x}_{\perp}(t) - \alpha(t)x_r(t) &= \dot{\underline{x}}_r(t) \sin \theta(t) + \dot{\underline{x}}_{\perp}(t) \cos \theta(t). \end{aligned} \quad (21)$$

Written in terms of $\underline{x}_r(t)$ and $\underline{x}_{\perp}(t)$ the semiclassical action of Eq. (17) becomes

$$S_{\gamma_c}^{sc}(\gamma) = \int_0^{\tau(\gamma_c, E)} dt \mathcal{L}_{\gamma_c}(\underline{x}_r, \dot{\underline{x}}_r, \underline{x}_{\perp}, \dot{\underline{x}}_{\perp}; E, t), \quad (22)$$

where the two-dimensional Lagrangian,

$$\begin{aligned} \mathcal{L}_{\gamma_c}(\underline{x}_r, \dot{\underline{x}}_r, \underline{x}_{\perp}, \dot{\underline{x}}_{\perp}; E, t) &= E + \frac{m_E}{2} (\dot{\underline{x}}_r^2(t) + \dot{\underline{x}}_{\perp}^2(t)) \\ &\quad - V_E[\underline{x}_r(t) \cos \theta(t) - \underline{x}_{\perp}(t) \sin \theta(t); t], \end{aligned} \quad (23)$$

contains an explicitly time-dependent potential term

$$V_E[z; t] = E \begin{cases} -z/R(t) & , \text{ if } z \geq 0 \text{ and } 0 < R(t) < \infty \\ \infty & , \text{ if } z < 0 \text{ and } 0 < R(t) < \infty \\ 0 & , \text{ otherwise,} \end{cases} \quad (24)$$

that vanishes at times t for which the classical path does not lie on the surface \mathcal{F} .

2.2 The Semiclassical Green function

The semiclassical action of Eq. (22) can be interpreted as describing the non-relativistic motion of a particle of mass $m_E = E/v^2(E)$ in a homogeneous but time-dependent gravitational-like potential in two dimensions. To complicate matters there is a (generally time-dependent) restriction that $x_r(t) = \underline{x}_r(t) \cos \theta(t) + \underline{x}_\perp(t) \sin \theta(t) \geq 0$ whenever $0 < R(t) < \infty$. In analogy to motion in a gravitational field, the restriction $x_r(t) \geq 0$ will be referred to as due to a (time-dependent) *ceiling*. Since the force is always directed *away* from the ceiling, there is *no classical trajectory* that starts from the ceiling and ends at the ceiling after a finite time $\tau(\gamma_c, E)$. However, the quantum mechanical amplitude for again observing the particle at the ceiling after a time $\tau(\gamma_c, E)$ does not vanish. We now proceed to calculate this amplitude and thus describe diffraction semiclassically.

To simplify the notation, let us introduce the two-dimensional position- and momentum- vectors

$$\vec{x} = (\underline{x}_r, \underline{x}_\perp), \quad \vec{\pi} = (m_E \dot{\underline{x}}_r, m_E \dot{\underline{x}}_\perp) \quad (25)$$

to describe the motion of the particle in phase space. The semiclassical Hamiltonian H_{γ_c} of our two-dimensional problem depends on the classical path γ_c and is explicitly time dependent. It is given by a Legendre transformation of the Lagrangian of Eq. (23) and in the notation of Eq. (25) reads

$$H_{\gamma_c}(\vec{x}, \vec{\pi}; t) = \vec{\pi} \cdot \dot{\vec{x}} - \mathcal{L}_{\gamma_c} = \frac{\vec{\pi}^2}{2m_E} + V_E(x_r(\vec{x}, t); t) - E. \quad (26)$$

Note that the *parameter* E of this two-dimensional Hamiltonian also determines the zero of the energy scale. This constant is unimportant for the dynamics at a *given* value of E , but is relevant when comparing the phases of the amplitudes at different wave numbers. Upon quantization of the classical problem described by the Hamiltonian of Eq. (26), the amplitude that a particle in this two-dimensional world found initially at the transverse deviation $\vec{x} = \vec{a}$ from the classical path will appear with transverse deviation $\vec{x} = \vec{b}$ a time $\tau(\gamma_c, E)$ later is the causal Green function

$$\begin{aligned} \mathcal{G}_{\gamma_c}(\vec{a}, \vec{b}; \tau(\gamma_c, E)) &= \langle \vec{b} | \exp \left\{ -\frac{i}{\hbar} \int_0^{\tau(\gamma_c, E)} dt \hat{H}_{\gamma_c}(\vec{x}, \vec{\pi}; t) \right\} | \vec{a} \rangle \\ &= \int_{\gamma} [dx] \exp \frac{i}{\hbar} S_{\gamma_c}^{sc}(\gamma). \end{aligned} \quad (27)$$

The (time-ordered) exponential in Eq. (27) is the time-evolution operator generated by a time-dependent Hamiltonian for a fixed time interval – here $\tau(\gamma_c, E)$, for given E – and the paths γ in the latter representation of the Green function

as a path integral in coordinate space are described by their transverse deviations, \vec{a} at $t = 0$ and \vec{b} at $t = \tau(\gamma_c, E)$, from the classical path γ_c . (We use the notation \mathcal{G} and G for exact and semiclassical Green functions. Rather than introduce a new symbol, we choose to write \mathcal{G}_{γ_c} for the exact Green function to the semiclassical Hamiltonian of Eq. (26) for the classical path γ_c .)

The semiclassical energy Green function $G(\mathbf{X}, \mathbf{Y}; E)$ is proportional to the sum over all classical trajectories γ_c of the amplitudes, $\sum_{\gamma_c} \mathcal{G}_{\gamma_c}(\vec{a} = \vec{b} = 0; \tau(\gamma_c, E))$. As noted in Appendix A, the two Green functions are related[17] by a factor that depends only on the local *group* velocities $v_g(\mathbf{X}, E)$ and $v_g(\mathbf{Y}, E)$ at the endpoints of the classical trajectories,

$$G(\mathbf{X}, \mathbf{Y}; E) = \frac{1}{i\hbar \sqrt{v_g(\mathbf{X}, E)v_g(\mathbf{Y}, E)}} \sum_{\gamma_c} \mathcal{G}_{\gamma_c}(\vec{a} = \vec{b} = 0; \tau(\gamma_c, E)). \quad (28)$$

For a homogeneous medium, the group velocity in fact does not depend on the location outside \mathcal{V} and $v_g(\mathbf{X}, E) = v_g(\mathbf{Y}, E) = v_g(E)$ and Eq. (28) simplifies accordingly.

3 An Example: Diffraction by a Sphere in a Uniform Medium

To better understand the general case of Eq. (27), it is illustrative to consider the example of diffraction when the excluded volume \mathcal{V} is a sphere of radius R . The exact expressions for the Green functions are known for this case and their asymptotic expansion for large $kR = ER/(\hbar v(E))$ has been obtained[1, 5, 6]. Besides making contact with previous work, the spherical case also exhibits some analytical properties of the Green function \mathcal{G}_{γ_c} that are essential in the construction of the solution for a more general obstacle.

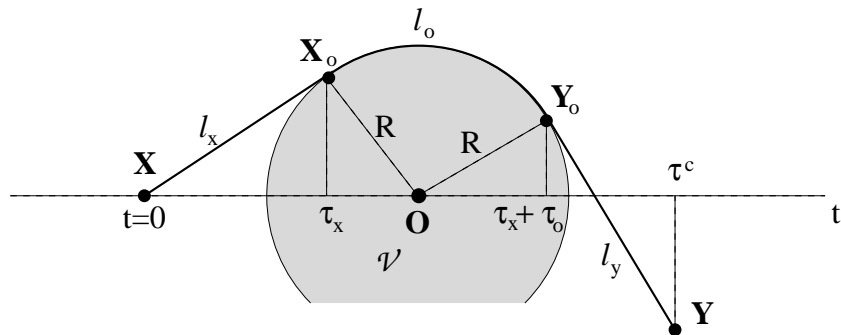


Fig. 2: The classical path, from \mathbf{X} at $t = 0$ to \mathbf{Y} at $t = \tau_c$ with winding number $w = +1$, for a spherical excluded volume \mathcal{V} of radius R . The path is planar and l_x and R fix the location of \mathbf{X} with respect to the center of the sphere, \mathbf{O} , and l_o and l_y then determine \mathbf{Y} . Note that for $|w| > 1$, the classical path would completely encircle the sphere. The phase velocity is $v(E)$, and $\tau_x = l_x/v(E)$, $\tau_o = l_o/v(E)$, $\tau_y = l_y/v(E)$, with $\tau_c = \tau_x + \tau_o + \tau_y$.

The initial point \mathbf{X} , the final point \mathbf{Y} and the center $\mathbf{0}$ of the sphere \mathcal{V} define a plane. Every classical trajectory lies wholly in this plane and the angle $\alpha(t)$ vanishes. As is evident from Fig. 2, classical trajectories in this case can be assigned an integer $w = 0, \pm 1, \pm 2 \dots$ that represents the number of times and the direction that the classical trajectory winds around the sphere in going from \mathbf{X} to \mathbf{Y} . $w = 0$ corresponds to the direct trajectory and does not occur if, for given \mathbf{X} , \mathbf{Y} lies in the shadow cast by the sphere. $w = \pm 1$ are the two trajectories of opposite winding sense that do touch the sphere but do not wind fully around it, $w = \pm 2$ is assigned to the two trajectories that wind once but not twice around the sphere, etc. . . . In addition to the sense in which it winds around the sphere, a classical trajectory γ_c is characterized by three lengths, l_x, l_o and l_y . l_x is the length of the straight line segment of the trajectory that is tangent to the sphere and extends from \mathbf{X} to a point \mathbf{X}_o on the surface of the sphere. Similarly l_y is the length of the straight line segment of the trajectory that is tangent to the sphere and extends from \mathbf{Y} to a point \mathbf{Y}_o on the surface of the sphere. Finally l_o denotes the length of the classical trajectory that “creeps” along the surface of the sphere between \mathbf{X}_o and \mathbf{Y}_o . The time intervals corresponding to these lengths are $\tau_x = l_x/v(E)$, $\tau_y = l_y/v(E)$ and $\tau_o = l_o/v(E)$, respectively, with

$$\tau_c = \tau(\gamma_c, E) = \tau_x + \tau_o + \tau_y . \quad (29)$$

It is not difficult to ascertain that such a trajectory is of extremal length.

The Green function $\mathcal{G}_{\gamma_c}(\vec{a} = \vec{b} = 0; \tau_c)$ is a function of the parameters $E, v(E), R$ and of the variables τ_x, τ_y, τ_o describing the classical path. Since $\alpha(t) = 0$, it follows that $\underline{x}_r = x_r$ and that $\underline{x}_\perp = x_\perp$. The potential in Eq. (26) therefore does not depend on x_\perp . The hamiltonian of Eq. (26) in this case is of the form

$$H_{\gamma_c} = H_\perp(\pi_\perp) + H_r(x_r, \pi_r; t) - E , \quad (30)$$

and the dynamics of the perpendicular and radial degrees of freedom separates. The time-independent Hamiltonian

$$H_\perp(\pi_\perp) = \frac{\pi_\perp^2}{2m_E} \quad (31)$$

describes the one-dimensional motion of a free non-relativistic particle of mass $m_E = E/v^2(E)$, whereas

$$H_r(x_r, \pi_r; t) = \frac{\pi_r^2}{2m_E} + V_E(x_r; t) \quad (32)$$

governs the radial dynamics. The boundary conditions $\vec{a} = \vec{b} = 0$ imply that $x_r(0) = x_r(\tau_c) = 0$ and $x_\perp(0) = x_\perp(\tau_c) = 0$. By virtue of the form of Eq. (30), the Green function $\mathcal{G}_{\gamma_c}(\vec{a} = \vec{b} = 0; \tau_c)$ decomposes into the product of two Green functions and an exponential, and we can write

$$\mathcal{G}_{\gamma_c}(\vec{0}, \vec{0}; \tau_c) = \exp(iE\tau_c/\hbar) \mathcal{G}_0(0, 0; \tau_c) \mathcal{G}_r(0, 0; \tau_c) , \quad (33)$$

where, for arbitrary x , y and τ ,

$$\mathcal{G}_0(x, y; \tau) = \sqrt{\frac{m_E}{2\pi i \hbar \tau}} \exp\left(\frac{im_E(x-y)^2}{2\hbar\tau}\right) \quad (34)$$

is the Green function for a free non-relativistic particle of mass m_E in one dimension and

$$\mathcal{G}_r(x, y; \tau) = \langle y | \exp\left\{-\frac{i}{\hbar} \int_0^\tau dt \hat{H}_r(x, \pi; t)\right\} | x \rangle \quad (35)$$

is the Green function corresponding to the time-evolution generated by the radial Hamiltonian of Eq. (32). The exponential factor in Eq. (33) originates in the $-E$ term in Eq. (30) and is the phase associated with the classical path. The explicit time dependence of the radial Hamiltonian in the case of a sphere is quite simple since the curvature of a classical path γ_c is of the form

$$\frac{1}{R(t)} = \begin{cases} 1/R & , \quad \tau_x < t < \tau_x + \tau_o \\ 0 & , \quad \text{otherwise} \end{cases} . \quad (36)$$

In the time intervals $[0, \tau_x]$ and $[\tau_x + \tau_o, \tau_x + \tau_o + \tau_y]$ the Hamiltonian of Eq. (32) describes the time evolution of a free non-relativistic particle of mass m_E . If the radial coordinate states were complete, \mathcal{G}_r could be further decomposed as

$$\begin{aligned} \mathcal{G}_r(0, 0; \tau_c) &= \int_0^\infty da \int_0^\infty db \mathcal{G}_0(0, a; \tau_x) \mathcal{G}_R(a, b; \tau_o) \mathcal{G}_0(b, 0; \tau_y) \\ &= \frac{k}{2\pi i} \int_0^\infty \frac{da}{\sqrt{l_x}} \int_0^\infty \frac{db}{\sqrt{l_y}} \mathcal{G}_R(a, b; \tau_o) \exp\left(\frac{ika^2}{2l_x} + \frac{ikb^2}{2l_y}\right) , \end{aligned} \quad (37)$$

where we used Eq. (34) in the latter expression. Here a and b denote the radial deviations of γ from γ_c at the points \mathbf{X}_o and \mathbf{Y}_o of Fig. 2. We will see in Sec. 4.4 that the propagation to a point at the surface of the obstacle is only approximately described by the free Green function. (Roughly speaking, a photon with large but finite k effectively penetrates a small distance into the sphere.) The *assumption* that \mathcal{G}_r separates in the form of Eq. (37) neglects subleading terms of the asymptotic expansion in the penumbra.

\mathcal{G}_R is the coordinate representation of the time evolution operator generated by the time-independent Hamiltonian

$$H_R(\pi, x) = \frac{\pi^2}{2m_E} - \frac{E}{R}x \quad (38)$$

in the half-space $x > 0$. The integrals over a and b in Eq. (37) extend only from zero to infinity because $\mathcal{G}_R(a, b; \tau)$ vanishes whenever either a or b are negative. We recognize that the one-dimensional quantum mechanical problem described by Eq. (38) is the propagation of a non-relativistic particle of mass $m_E = E/v^2(E)$ under the influence of a constant force leading to an acceleration

$|g| = v^2(E)/R$ directed *away* from $x = 0$. Note that $\mathcal{G}_R(x, y; \tau) = \mathcal{G}_R^*(y, x; -\tau)$, because the Hamiltonian Eq. (38), although not bounded below, is hermitian. By definition, the causal Green function \mathcal{G}_R satisfies the second order differential equation

$$-\left(\frac{\hbar^2}{2m_E} \frac{\partial^2}{\partial x^2} + \frac{Ex}{R}\right) \mathcal{G}_R(x, y; \tau) = i\hbar \frac{\partial}{\partial \tau} \mathcal{G}_R(x, y; \tau) \quad (39)$$

in the half-space $x > 0, y > 0$ and the initial condition

$$\mathcal{G}_R(x, y; 0) = \delta(x - y) . \quad (40)$$

The solution to Eq. (39) and Eq. (40) is completely specified by imposing the boundary conditions

$$\mathcal{G}_R(0, y; \tau) = 0 \quad \text{and} \quad \lim_{x \rightarrow \infty} \mathcal{G}_R(x, y; \tau) = 0 , \quad (41)$$

and requiring that the magnitude of \mathcal{G}_R remain bounded for $\tau \rightarrow \infty$

$$|\mathcal{G}_R(x, y; \tau \rightarrow \infty)| < \infty . \quad (42)$$

The latter condition excludes any solution which increases exponentially and is just the requirement that the presence of an obstacle should not lead to the *production* of photons in the shadowed region.

3.1 The spectral representation of \mathcal{G}_{-R}

The Hamiltonian (38) is hermitian and bounded below only for *negative* values of the parameter R . In this case it can be interpreted as describing a non-relativistic particle in a homogenous gravitational field in the half-space $x > 0$ above a table. The spectral representation of the solution to Eqs. (39) and (40) that satisfies the boundary conditions in Eqs. (41) and (42) is well known[16]. Our strategy is as follows. For $R > 0$ waves diffract and there are no classical orbits, while for $R < 0$ there are classical orbits, a much simpler situation. We will therefore analyze the $R > 0$ case by first considering the $R < 0$ case, and then return to the $R > 0$ case of interest by analytic continuation.

With R replaced by $-R$, we have

$$\mathcal{G}_{-R}(x, y; \tau_o) = \frac{k}{\sigma R} \sum_{n=0}^{\infty} \Psi_n(x) \Psi_n(y) \exp(-i\tau_o v(E) \epsilon_n \sigma) , \quad (43)$$

where the inverse length scale σ is

$$\sigma = \frac{k}{2^{1/3} (kR)^{2/3}} , \quad (44)$$

and the wave function

$$\Psi_n(x) = \text{Ai}\left(\frac{kx}{\sigma R} - \epsilon_n\right) / |\text{Ai}'(-\epsilon_n)| \quad (45)$$

is given by the Airy function[18] and its derivative, $\text{Ai}'(z) = (d/dz)\text{Ai}(z)$. Considered as a function on the complex plane, the Airy function $\text{Ai}(z)$ is the solution to the differential equation

$$\frac{d^2}{dz^2}\text{Ai}(z) = z\text{Ai}(z) \quad (46)$$

with the asymptotic behavior for $|z| \rightarrow \infty$,

$$\begin{aligned} \text{Ai}(z) &\sim \frac{1}{2\sqrt{\pi}}z^{-1/4}\exp(-\frac{2}{3}z^{3/2}), \quad |\arg z| < \pi \\ \text{Ai}(-z) &\sim \frac{1}{\sqrt{\pi}}z^{-1/4}\sin(\frac{2}{3}z^{3/2} + \frac{\pi}{4}), \quad |\arg z| < \frac{2\pi}{3}. \end{aligned} \quad (47)$$

The first of the boundary conditions of Eq. (41) relates the ϵ_n 's to the zero's of the Airy function

$$\text{Ai}(-\epsilon_n) = 0, \quad n = 0, 1, \dots \quad (48)$$

Since the zero's of the Airy function are all on the negative real axis[18], the ϵ_n are real and positive and are ordered as $0 < \epsilon_n < \epsilon_{n+1}$. That $\text{Ai}'(-\epsilon_n)$ gives the proper normalization of the wave functions follows from the identity,

$$\int_z^\infty dx \text{Ai}^2(x) = (\text{Ai}'(z))^2 - z\text{Ai}^2(z). \quad (49)$$

Eq. (49) is proven by taking the derivative of both sides and using Eq. (46). Choosing $z = -\epsilon_n$ in Eq. (49), dividing by $[\text{Ai}'(-\epsilon_n)]^2$, and redefining the integration variable as $x \rightarrow \sigma x - \epsilon_n$, one finds that $\int_0^\infty dx \Psi_n^2(x) = 1/\sigma$. Since the Ψ_n are eigenfunctions of a hermitian operator corresponding to the eigenvalue ϵ_n , Ψ_n and Ψ_m are orthogonal for $n \neq m$ and therefore,

$$\int_0^\infty dx \Psi_n(x)\Psi_m(x) = \delta_{nm}/\sigma. \quad (50)$$

The completeness of the spectrum of the bounded hermitian operator H_{-R} in the space of normalizable functions on the half space $x > 0$ that vanish at $x = 0$, together with Eq. (50), proves that Eq. (43) also fulfills Eq. (40). Thus the spectral representation Eq. (43) would be the (unique) solution of Eq. (39) and Eq. (40) we are looking for *if* the parameter R in Eq. (39) were negative.

3.2 The spectral representation of \mathcal{G}_R by analytic continuation

To obtain the spectral representation of \mathcal{G}_R for *positive real* values of R , we analytically continue \mathcal{G}_{-R} in the complex plane. With R the modulus of the complex number R_ϕ ,

$$R_\phi = Re^{i\phi}, \quad (51)$$

the analytic continuation of the spectral representation Eq. (43) \mathcal{G}_{-R_ϕ} in the phase ϕ is uniquely given by requiring that Eq. (42) hold for all $0 \leq \phi \leq \pi$. The dependence of the inverse scale factor σ on the phase is

$$\sigma_\phi = \sigma e^{-2i\phi/3} . \quad (52)$$

For sufficiently large positive values of x , $-\frac{\pi}{3} < \arg(kx/(\sigma_\phi R_\phi) - \epsilon_n) \leq 0$ for any fixed n and the Airy function decays exponentially as given in Eq. (47). Note, however, that the behavior of the wave functions for large arguments becomes oscillatory with a power-law decay at the endpoint $\phi = \pi$ of the interval. This is consistent with the fact that there is only one turning point of a trajectory with fixed energy in this case. The boundary conditions Eq. (41) thus hold for all $\phi \in [0, \pi]$. Finally, because

$$\text{Im}\sigma_\phi < 0 \text{ for } 0 < \phi \leq \pi , \quad (53)$$

the Green function of Eq. (43) *decays* for large times τ and Eq. (42) holds. Note that the only dependence of \mathcal{G}_R on the arc length l_o of the creeping section of the trajectory is via $\tau = \tau_o = l_o/v(E)$. \mathcal{G}_R thus decays exponentially with the length l_o of the creeping section with an exponent that is proportional to $l_o(kR)^{1/3}/R$. This dependence of the exponent on the cube root of the wave number is somewhat unusual and perhaps unexpected for a semiclassical expansion, but is typical for diffraction[1]. Setting $\phi = \pi$ in Eq. (43), $R \rightarrow R_\pi = -R$ and therefore $\sigma \rightarrow \sigma_\pi \equiv \bar{\sigma}$, where

$$\bar{\sigma} = \frac{ke^{-2\pi i/3}}{2^{1/3}(kR)^{2/3}} . \quad (54)$$

Using Eqs. (43) and (45), one thus finally obtains

$$\mathcal{G}_R(x, y; \tau_o) = \mathcal{G}_{-R_\pi}(x, y; \tau_o) = \frac{-k}{\bar{\sigma}R} \sum_{n=0}^{\infty} \frac{\text{Ai}(-\frac{kx}{\bar{\sigma}R} - \epsilon_n) \text{Ai}(-\frac{ky}{\bar{\sigma}R} - \epsilon_n)}{[\text{Ai}'(-\epsilon_n)]^2} e^{-i\bar{\sigma}l_o\epsilon_n} , \quad (55)$$

as the spectral representation of the Green function that satisfies Eqs. (39) and (40) as well as the boundary conditions Eqs. (41) and (42).

Inserting Eq. (55) in Eq. (37), \mathcal{G}_r is found to have the representation

$$\mathcal{G}_r(0, 0; \tau_c) = \frac{ik}{4\pi\bar{\sigma}R} \sum_{n=0}^{\infty} \mathcal{D}_n(\bar{\sigma}l_x) \mathcal{D}_n(\bar{\sigma}l_y) e^{-i\bar{\sigma}l_o\epsilon_n} , \quad (56)$$

with amplitudes

$$\mathcal{D}_n(\xi) = \int_0^\infty d\rho \frac{\text{Ai}(\rho\sqrt{\xi} - \epsilon_n)}{|\text{Ai}'(-\epsilon_n)|} \exp\left(\frac{i\rho^2}{4}\right) , \quad (57)$$

the result previously obtained[2] for the asymptotic behavior in the deep shadow region. Within the semiclassical approximation it might appear to be consistent to further approximate the Airy function and its zeros semiclassically and

evaluate the integral in Eq. (57) in saddle point approximation. This is done in Appendix B and indeed was part of the original approach[1, 2]. However, although perfectly reasonable, one should perhaps point out that it is not simple to justify this procedure from the *semiclassical* point of view: the error of the semiclassical approximation is largest for the *lowest* zeros of the Airy function, which apparently dominate the sum in Eq. (56) in the semiclassical limit. An alternative to the semiclassical approximation of the spectral representation of the Green function and associated integrals is the direct semi-classical evaluation of the path-integral discussed below. It gives corrections to the above procedure that become important outside the deeply shadowed region.

4 Diffraction by a Sphere: Semiclassical Evaluation of the Path Integral

In the previous section we constructed the *exact* spectral representation, given by Eqs. (56) and (57), of the Green-function Eq. (35) for the radial motion by analytic continuation. At the end of the calculation we argued that the semiclassical approximation of the zeros, ϵ_n , and of the remaining integrals \mathcal{D}_n may not be fully justified. We now proceed to do the calculation in reverse; we first obtain the semiclassical approximation to \mathcal{G}_r for negative values of the parameter R and *then* analytically continue the semiclassical result to positive values of R . Although this procedure is of only pedagogical value in the case of a sphere[19], it has the great advantage of being generalizable to more complex situations. We will see that this method of evaluation is also interesting for conceptual reasons.

The point is that there *are* classical trajectories for the radial motion from x to y in time τ *if* the parameter R in the definition Eq. (24) of the potential $V_E(x_r; t)$ of the Hamiltonian H_r given in Eq. (32) is negative. In this case the force on the particle is either absent or directed toward the endpoint at $x_r = 0$. The force of magnitude E/R is turned on at “time” τ_x and lasts only for a finite time τ_o . Using the horizontal axis to denote the time and the vertical one to denote the “height” $x(t)$, the classical trajectory during the time interval τ_o is that of a ball bouncing up and down vertically on a table. See Fig. 3. There are many classical trajectories that start with an initial height $x(0) = x$ and which, at $\tau_c = \tau_x + \tau_o + \tau_y$, attain a final height $x(\tau_c) = y$. They are distinguished by the number of bounces[20], $n = 0, 1, 2, \dots$. If the initial or final point are above the table, the classification of a classical trajectory by the number of bounces is not unique. There are classical trajectories with the same number of bounces that differ in the directions of the initial and/or final momentum. The ambiguity for a given n is at most 4-fold. If $x \leq 0$ and $y \leq 0$, this ambiguity is removed since the ball has to be above the table in the intermediate region. The signs of the initial and final momenta must be positive and negative, respectively, and the classification of a classical trajectory by the number n is unique. Eventually we are interested only in trajectories that start and end level with the table. To

avoid unnecessary (and irrelevant) complications, we consider only the situation where the initial and final points satisfy $x \leq 0$ and $y \leq 0$, that is, are below or level with the table.

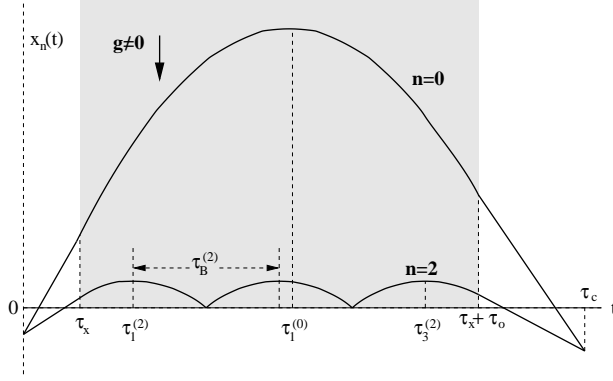


Fig. 3: Radial deviations with $n = 0$ (no bounces) and $n = 2$ (two bounces) from a particular classical path γ_c for a spherical obstacle of radius R . In the time intervals $[0, \tau_x]$ and $[\tau_x + \tau_o, \tau_c]$, there is no acceleration and these sections of the paths are straight lines; the motion in the interval $[\tau_x, \tau_x + \tau_o]$ is governed by a constant acceleration $g = -v^2(E)/R$. The initial and final radial deviations from γ_c , $x = x_n(0)$ and $y = x_n(\tau_c)$, not labeled in the figure, do not depend on n . $\tau_i^{(n)}$ is the i -th turning point of the path with n bounces, $\tau_B^{(n)}$ is the time between successive bounces, or successive turning points.

The classical trajectory γ_n connecting x and y in time τ_c with n bounces is a piecewise connected solution to the equation of motion

$$\ddot{x}_n(t) = -g(t) \quad (58)$$

with $x(0) = x$ and $x(\tau_c) = y$ and $x(t) \geq 0$ for $\tau_x < t < \tau_x + \tau_o$ that apart from the n points corresponding to bounces is continuous in phase space. Since the (negative) acceleration $g(t) = v^2(E)/R = g$ does not depend on time in the interval $\tau_x < t < \tau_x + \tau_o$, the “energy” (for notational convenience we extract the scale to have a dimensionless energy)

$$e_n = \frac{2}{m_E g R} \left(\frac{\pi_n^2(t)}{2m_E} + m_E g x_n(t) \right) = \frac{\pi_n^2(t)}{(\hbar k)^2} + 2 \frac{x_n(t)}{R}, \quad (59)$$

is a real positive constant of motion that characterizes the trajectory in this time interval. In the initial and final time intervals $t \in [0, \tau_x]$ and $t \in [\tau_x + \tau_o, \tau_c]$ the acceleration vanishes and the momenta are constant. We also introduce dimensionless initial and final “momenta”,

$$\begin{aligned} p_n &= \pi_n(0)/(\hbar k) = \pi_n(\tau_x)/(\hbar k) > 0, \\ p'_n &= -\pi_n(\tau_c)/(\hbar k) = -\pi_n(\tau_x + \tau_o)/(\hbar k) > 0. \end{aligned} \quad (60)$$

The signs have been chosen so that p_n and p'_n are both positive for initial and final points $x \leq 0$ and $y \leq 0$. The equation of motion (58) with $g(t) = 0$ implies

that

$$x_n(\tau_x) = x + l_x p_n \quad \text{and} \quad x_n(\tau_x + \tau_o) = y + l_y p'_n . \quad (61)$$

Demanding continuity of the classical trajectory in phase space at $t = \tau_x$ and $t = \tau_x + \tau_o$, we determine p_n and p'_n in terms of e_n . They are given by

$$\begin{aligned} p_n &= \sqrt{e_n + (l_x/R)^2 - 2x/R} - l_x/R \\ p'_n &= \sqrt{e_n + (l_y/R)^2 - 2y/R} - l_y/R . \end{aligned} \quad (62)$$

The signs of the square roots have been chosen so that both scaled momenta, p_n and p'_n , are positive for initial and final heights $x \leq 0$ and $y \leq 0$.

To completely specify the trajectory, we need an equation for e_n . The acceleration is constant for $\tau_x < t < \tau_x + \tau_o$ and the first turning point of the trajectory occurs at $t = \tau_1^{(n)}$, where

$$\tau_1^{(n)} = \tau_x + p_n R/v(E) . \quad (63)$$

The last turning point, the $(n+1)^{\text{th}}$, occurs at $t = \tau_{n+1}^{(n)}$, where

$$\tau_{n+1}^{(n)} = \tau_x + \tau_o - p'_n R/v(E) . \quad (64)$$

The equation of motion (58) for constant acceleration finally relates the time $\tau_B^{(n)}$ between successive bounces (or successive turning points) when there are n bounces in all to the conserved "energy" e_n ,

$$\tau_B^{(n)} = 2\sqrt{e_n} R/v(E) . \quad (65)$$

The time to the first turning point plus the time for n bounces plus the time from the last turning point to the end of the trajectory is the total time τ_c of the trajectory. We thus have that $\tau_1^{(n)} + n\tau_B^{(n)} + (\tau_c - \tau_{n+1}^{(n)}) = \tau_c$, or

$$p_n + p'_n + 2n\sqrt{e_n} = l_o/R . \quad (66)$$

Eq. (66) together with Eq. (62) is a fourth order algebraic equation for e_n whose roots can be found analytically. There is only one real and positive solution e_n , because the left hand side of Eq. (66) is a monotonically increasing function of e_n that vanishes at $e_n = 0$ and goes as $2(n+1)\sqrt{e_n}$ for large values of e_n . We remark that e_n, p_n and p'_n given by Eq. (66) and Eq. (62) depend only on the lengths l_x, l_o and l_y of the problem and the scaled initial and final heights x and y (all measured in units of R). The solution e_n of Eq. (66) therefore does not depend on E nor $v(E)$. The action $S_n(x, y)$ of the classical trajectory with n bounces is proportional to $ER/v(E) = \hbar kR$. After some algebra, $S_n(x, y)$ can be expressed in terms of e_n, p_n and p'_n implicitly given by Eq. (66) and Eq. (62). We find

$$\frac{S_n(x, y)}{\hbar k R} = \frac{p_n^3 + p_n'^3 + 2ne_n^{3/2}}{3} + \frac{p_n^2 l_x + p_n'^2 l_y - e_n l_o}{2R} . \quad (67)$$

Using Eq. (62), one explicitly verifies that

$$\frac{\partial S_n(x, y)}{\partial e_n} = \frac{\hbar k R}{2} (p_n + p'_n + 2n\sqrt{e_n} - l_o/R) . \quad (68)$$

Eq. (66) thus selects the energy e_n at which the action is stationary. This fact will be of some consequence when we compare the present approach to the one of section 3.

The semiclassical approximation $G_r(x, y; \tau_c, -R)$ to the Green function $\mathcal{G}_r(x, y; \tau_c, -R)$ defined in Eq. (35) might *seem* to be the sum of the asymptotic contributions from the infinite number of classical path. The semiclassical contribution of a single classical path is known; it is given by Van Vleck's formula[21]. *If* we could simply sum over the asymptotic contributions of all classical trajectories, we would (in this one dimensional case) obtain

$$G_r(0, 0; \tau_c, -R) = \frac{1}{\sqrt{2\pi i \hbar}} \sum_{n=0}^{\infty} \sqrt{\frac{-\partial^2 S_n(x, y)}{\partial x \partial y}} \Big|_{x=y=0} \exp i \left(\frac{S_n(0, 0)}{\hbar} - \frac{3\pi n}{2} \right) . \quad (69)$$

(There are n conjugate points and n points of reflection on the classical trajectory with n bounces, contributing in total a phase factor of $\exp(-i3\pi n/2)$.)

Although each term of the sum is the correct asymptotic contribution from a *particular* classical trajectory, we now show that Eq. (69) does *not* give the asymptotic behavior of the Green function \mathcal{G}_r for $kR \rightarrow \infty$. The cause of the problem is that for any fixed value of kR , the classical trajectories and their corresponding action S_n become indistinguishable as $n \rightarrow \infty$. The "floor" at $x = 0$ is a zero-dimensional caustic of the classical motion[14]. It then is not possible to interchange the implicit $kR \rightarrow \infty$ limit with the sum over n in Eq. (69).

To see that the interchange is not allowed, we examine the asymptotic behavior of the classical action S_n for trajectories with large n , assuming for the moment that Eq. (69) is valid. We begin by observing that the second derivatives of the action appearing in Eq. (69) can be evaluated in terms of the solutions p_n, p'_n and e_n of Eq. (66) and Eq. (62) for $x = y = 0$. The classical equations of motion imply that the initial momentum $\pi_n(0)$ is given by

$$\frac{\partial S_n(x, y)}{\partial x} = -\pi_n(0) = -\hbar k p_n . \quad (70)$$

Eq. (70) can be checked explicitly by taking the derivative of Eq. (67) and using Eqs. (62) and (66). From Eq. (70) we thus have that

$$-\frac{\partial^2 S_n(x, y)}{\partial x \partial y} \Big|_{x=y=0} = \hbar k \frac{\partial p_n}{\partial y} \Big|_{x=y=0} . \quad (71)$$

The variation of the initial momentum with the endpoint of the trajectory required in the latter expression is implicitly given by Eq. (66) and the defini-

tions Eq. (62). After some algebra we obtain

$$-\frac{\partial^2 S_n(x, y)}{\partial x \partial y} = \frac{\hbar k e_n}{l_o(p_n + \frac{l_x}{R})(p'_n + \frac{l_y}{R}) + p_n l_x(p'_n + \frac{l_y}{R}) + p'_n l_y(p_n + \frac{l_x}{R})}. \quad (72)$$

Note that in Eq. (69) we need only know the right hand side of Eq. (72) at $x = y = 0$. To evaluate the function Eq. (69) it thus is sufficient to solve Eq. (66) with $x = y = 0$.

The solution e_n of Eq. (66) will be small compared to either l_x^2/R^2 or l_y^2/R^2 when n is sufficiently large. For $x = y = 0$, we then may expand the roots occurring in Eq. (62) and thus solve Eq. (66) asymptotically for large n with the result

$$\sqrt{e_n} = \frac{1}{2n} (l_o/R) + O(n^{-3}, x/l_x, y/l_y). \quad (73)$$

The scaled momenta p_n and p'_n defined by Eq. (62) therefore are of order n^{-2} and

$$-\frac{\partial^2 S_n(x, y)}{\partial x \partial y} \Big|_{x=y=0} = \frac{\hbar k l_o}{4l_x l_y n^2} + O(n^{-4}). \quad (74)$$

Note that in this limit

$$S_n(0, 0) = -\frac{\hbar k l_o^3}{24R^2 n^2} + O(n^{-4}) \quad (75)$$

depends neither on l_x nor on l_y . This is readily understood. For n bounces within a given time interval τ_c , their height becomes exceedingly small compared to l_x or l_y . For $x = y = 0$ and large n , the initial and final momenta of the trajectory are of order n^{-2} and the free sections of the trajectory therefore do not contribute appreciably to the classical action. One can check that Eq. (75) indeed is just the action for a classical trajectory with n bounces that altogether take a time $\tau_o = l_o/v(E)$. The asymptotic behavior in Eqs. (74) and (75) implies that the sum in Eq. (69) converges to a logarithm for large n .

The asymptotic form Eq. (75), however, also shows that the actions of classical trajectories differ by much less than \hbar for $n \gg \sqrt{kR}$. For a fixed value of kR , the classical paths with sufficiently large n therefore could (and should) be considered quantum fluctuations of each other. It becomes a matter of exchanging limits: the asymptotic weight of a particular classical path characterized by n bounces in the limit $kR \rightarrow \infty$ is indeed given by its contribution to Eq. (69). However, we actually would like to know how the (infinite) sum of classical paths contribute to the Green function for a large, but fixed value of kR . The problem arises because the trajectory $\lim_{n \rightarrow \infty} x_n(t) = x_\infty(t) = 0$ is a caustic that is approached by an infinite number of classical trajectories. Note, however, that the sum in Eq. (69) would be cut off at a finite value $n = n_{max}$ for a *negative* value of the initial point x or final point y . Due to the non-vanishing initial and/or final momentum, the “energy” e_n of a trajectory in this case is bounded from below, $e_n \geq \text{Max}((x/l_x)^2, (y/l_y)^2)$, and Eq. (66) can be solved only for $n \leq n_{max}$. Eq. (69) in this case *would* give the correct asymptotic expression for sufficiently large kR .

For a given geometry and wave number k , successive terms of the sum in Eq. (69) tend to interfere destructively for sufficiently high n – one thus should reorder the sum and collect terms of similar phase. To do so, we make use of our earlier observation in Eq. (68) that Eq. (66) gives the stationary point of S_n with respect to a variation of the “energy” e_n . The second derivative of the action at this stationary point is

$$\begin{aligned} \frac{\partial^2 S_n(0,0)}{\partial e_n^2} &= \frac{\hbar k R}{4} \left(\frac{1}{p_n + l_x/R} + \frac{1}{p'_n + l_y/R} - \frac{p_n + p'_n - l_o/R}{e_n} \right) \Big|_{x=y=0} \\ &= \frac{\hbar k [l_o(p_n + \frac{l_x}{R})(p'_n + \frac{l_y}{R}) + p_n l_x (p'_n + \frac{l_y}{R}) + p'_n l_y (p_n + \frac{l_x}{R})]}{4e_n(p_n + l_x/R)(p'_n + l_y/R)} \Big|_{x=y=0} > 0 \end{aligned} \quad (76)$$

where we have used the definitions (62) to write the numerator in terms of p_n and p'_n only.

We will show just below that it is consistent, within the semiclassical approximation, to replace Eq. (69) by the integral expression

$$G_r(0,0; \tau_c, -R) = \frac{-i}{\pi \hbar} \int_0^\infty e \, de \, B(e) e^{iS(e)/\hbar} \sum_{n=0}^\infty e^{inf(e)} , \quad (77)$$

where

$$f(e) = \frac{2kR}{3} e^3 - \frac{3\pi}{2} . \quad (78)$$

In Eq. (77) the factor $B(e)$ is given by Eqs. (72) and (76) with e_n replaced by e^2 , that is,

$$\begin{aligned} B(e) &= \sqrt{\frac{-\partial^2 S_n(x,y)}{\partial x \partial y} \frac{\partial^2 S_n(x,y)}{\partial e_n^2}} \Big|_{x=y=0; e_n=e^2} \\ &= \frac{\hbar k}{2 [(e^2 + (l_x/R)^2)(e^2 + (l_y/R)^2)]^{1/4}} , \end{aligned} \quad (79)$$

and $S(e)$ is related to the action of Eq. (67),

$$S(e) = \hbar k R \left(\frac{p^3 + p'^3}{3} + \frac{p^2 l_x + p'^2 l_y - e^2 l_o}{2R} \right) , \quad (80)$$

where here too e_n has been replaced by e^2 . In addition the only explicitly n -dependent term in $S_n(x,y)$ of Eq. (67) has been separated out. In Eqs. (79) and (80) the variables p and p' are the dimensionless initial and final momenta of Eq. (62) for $x = y = 0$ and “energy” e^2 , that is

$$p = \sqrt{e^2 + (l_x/R)^2} - l_x/R , \quad p' = \sqrt{e^2 + (l_y/R)^2} - l_y/R . \quad (81)$$

To show the semiclassical equivalence of Eqs. (69) and (77), recall that the phase of the integrand in Eq. (77) for a given n is stationary at $e = \sqrt{e_n}$.

Expanding about $e = \sqrt{e_n}$, and evaluating the resultant Gaussian integral, one finds that Eqs. (69) and (77) are indeed equivalent term by term.

The asymptotic contribution of a classical path with a given n to the Green function in Eq. (77) thus is precisely the same as in Eq. (69). On the other hand we now can interchange the limits and obtain the correct asymptotic expansion by summing the geometrical series in Eq. (77) for a given value of kR . With a small positive imaginary component of e , the sum in Eq. (77) is evaluated as

$$\lim_{\eta \rightarrow 0^+} \sum_{n=0}^{\infty} e^{in(f(e)+i\eta)} = \lim_{\eta \rightarrow 0^+} \frac{1}{1 - e^{i(f(e)+i\eta)}}. \quad (82)$$

The integrand of Eq. (77) therefore has simple poles just below the real axis at $f(e) = 2\pi m - i\eta$ for integer m . Apart from these simple poles, the integrand is analytic in the shaded region of Fig. 4. The integration over e in Eq. (77) along the real axis therefore is equivalent to integrating along the contours \mathcal{C}_{sd} and $\mathcal{C}_{\mathcal{R}}$ shown in Fig. 4 and including the residues from the enclosed poles. The paths \mathcal{C}_{sd} and $\mathcal{C}_{\mathcal{R}}$ in the complex plane are chosen so that, as shown below,

- i) the contribution from $\mathcal{C}_{\mathcal{R}}$ to the integral is negligible for sufficiently large \mathcal{R} , and
- ii) the modulus of the integrand in Eq. (77) decreases monotonically and as fast as possible along \mathcal{C}_{sd} , the path of steepest descent.

The semi-classical evaluation of the integral in Eq. (77) thus has three distinct contributions, to be denoted by G_{poles} , $G_{\mathcal{C}_{\mathcal{R}}}$ and $G_{\mathcal{C}_{sd}}$. We discuss them separately.

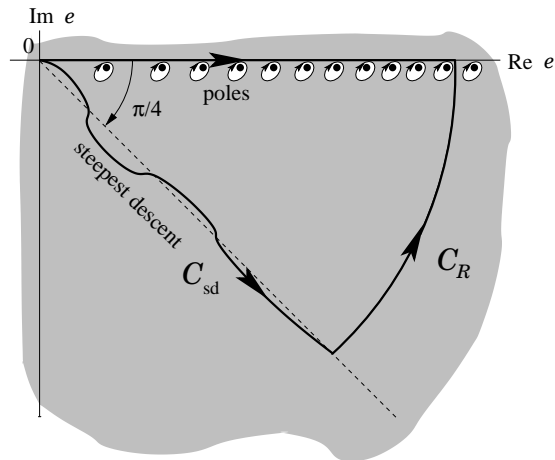


Fig. 4: Contours of integration. Apart from discrete poles just below the positive real axis, the integrand of Eq. (77) is analytic in the shaded region of the complex plane. The integral along the positive real axis in Eq. (77) from the origin to \mathcal{R} is evaluated by integrating along the contours \mathcal{C}_{sd} and $\mathcal{C}_{\mathcal{R}}$, taking the residues of the poles inside the closed contour into account. \mathcal{C}_{sd} is the path of steepest descent of the integrand that

starts at the origin. It asymptotically approaches the dashed line with $\arg e = -\pi/4$ for large $|e| \sim \infty$.

4.1 The Contribution from Poles with Integer $m \geq 0$

In the shaded region of the complex plane of Fig. 4, the integrand of Eq. (77) is analytic except for simple poles at

$$e = e(m) = \left(\frac{3\pi(m + 3/4)}{kR} \right)^{1/3} = \left(\frac{2}{kR} \right)^{1/3} \sqrt{\bar{\epsilon}_m}, \quad (83)$$

just below the real axis for any integer $m \geq 0$. Note that $\bar{\epsilon}_m$ corresponds to a semiclassical determination of the $(m + 1)^{\text{th}}$ zero ϵ_m of the Airy function[16]. The contribution $G_{\text{poles}}(-R)$ to $G_r(0, 0; \tau_c, -R)$ from the poles is

$$-2\pi i \sum_{m=0}^{\infty} \left\{ \begin{array}{l} \text{residue of} \\ \text{pole at } e(m) \end{array} \right\} = \frac{-i}{\hbar k R} \sum_{m=0}^{\infty} \frac{B(e(m))}{e(m)} e^{iS(e(m))/\hbar}. \quad (84)$$

Using Eqs. (44) (79), (81), (80) and (83), $G_{\text{poles}}(-R)$ can be rewritten as

$$G_{\text{poles}}(-R) = \frac{k}{4\pi i \sigma R} \sum_{n=0}^{\infty} D_n(\sigma l_x) D_n(\sigma l_y) e^{-i\sigma l_o \bar{\epsilon}_n}, \quad (85)$$

with diffraction amplitudes

$$D_n(\xi) = \frac{\sqrt{\pi}}{[\bar{\epsilon}_n(\bar{\epsilon}_n + \xi^2)]^{1/4}} \exp i \left(\frac{2\bar{p}_n^3(\xi)}{3} + \xi \bar{p}_n^2(\xi) \right). \quad (86)$$

The $D_n(\xi)$ depend on $\bar{\epsilon}_n$ defined by Eq. (83) and the corresponding (rescaled) "momenta"

$$\bar{p}_n(\xi) = \sqrt{\bar{\epsilon}_n + \xi^2} - \xi. \quad (87)$$

Since $\bar{p}_n(\xi) \sim e(n) \sim n^{1/3}$ for large n , the n^{th} and $(n + 1)^{\text{th}}$ contribution to the sum in Eq. (85) differ by a *finite* phase. By first summing in Eq. (77) rather than semiclassically evaluating the integral over e for each summand, one avoids the problem discussed earlier that for fixed wave number k , classical paths near a caustic interfere with one another. [Note that the individual summands of Eq. (85) do not correspond to contributions from individual classical paths of the original problem.]

The similarity between the expressions in Eqs. (85) and (56) is no coincidence. We show in Appendix B that apart from approximating the zero's of the Airy function ϵ_n by $\bar{\epsilon}_n$, D_n is proportional to the integral of Eq. (57) evaluated in saddle point approximation. We thus could have obtained the expression Eq. (85) by evaluating all integrals in saddle-point approximation and replacing the wave-functions $\Psi_n(x)$ and corresponding energies ϵ_n in Eq. (56) by their WKB counterparts. The fact that such a procedure ignores any asymptotic contribution from the integration along \mathcal{C}_{sd} and $\mathcal{C}_{\mathcal{R}}$ indicates that this may not be the whole story, and indeed it is not.

4.2 The Contribution $G_{\mathcal{C}_{\mathcal{R}}}$

The contribution to the Green function from integrating along the arc $\mathcal{C}_{\mathcal{R}}$ is negligible for sufficiently large \mathcal{R} . To see this, we use Eqs. (77)- (82) to write this contribution to G_r in the form

$$G_{\mathcal{C}_{\mathcal{R}}}(-R) = \frac{i}{\pi\hbar} \int_{\mathcal{C}_{\mathcal{R}}} e \, de B(e) \frac{e^{i[(S(e)/\hbar) - f(e)]}}{1 - e^{-if(e)}} , \quad (88)$$

where the contour $\mathcal{C}_{\mathcal{R}}$ is shown in Fig. 4.

Consider the behavior of the integrand in Eq. (88), with the contour $\mathcal{C}_{\mathcal{R}}$ chosen to be an arc of very large radius $\mathcal{R} = |e|$ centered on the origin that extends from the positive real axis into the lower half of the complex plane with $-\pi/3 < \arg e < 0$. The real part of $if(e)$ on the arc is positive and proportional to $|e|^3$. $e^{-if(e)}$ therefore is exponentially small on $\mathcal{C}_{\mathcal{R}}$ and for sufficiently large $\mathcal{R} = |e|$ is negligible compared to 1 – the denominator of the integrand thus approaches unity. To expand $(S(e)/\hbar) - f(e)$ for large $|e|$ and $-\pi/3 < \arg e < 0$, note that $p \sim e - l_x$ and $p' \sim e - l_y$ in this region. The leading e^3 term of $S(e)$ for $|e| \sim \infty$ is cancelled by the leading term of $f(e)$ and one has, for $|e| \sim \infty$ and $-\frac{\pi}{2} < \arg e < 0$,

$$(S(e)/\hbar) - f(e) \sim -\frac{k}{2}(l_x + l_y + l_o)e^2, \quad . \quad (89)$$

Since $\text{Re}(-ie^2) < 0$, Eq. (89) shows that the contribution of $\mathcal{C}_{\mathcal{R}}$ to the integral in Eq. (88) vanishes in the limit $\mathcal{R} \rightarrow \infty$.

4.3 The Contribution $G_{\mathcal{C}_{\text{sd}}}$

The contribution $G_{\mathcal{C}_{\text{sd}}}(-R)$ is given by Eq. (88), with $\mathcal{C}_{\mathcal{R}}$ replaced by \mathcal{C}_{sd} . The section \mathcal{C}_{sd} of the contour is chosen to coincide with the path of steepest descent that begins at the origin. From Eq. (89) we see that $\arg e$ along this path approaches $-\pi/4$ for very large values of $|e|$. Because p and p' are both proportional to e^2 for small $|e|$, the leading behavior in this limit is (using Eqs. (78) and (80))

$$(S(e)/\hbar) - f(e) \sim \frac{3\pi}{2} - \left[\frac{kl_o}{2}e^2 + \frac{2kR}{3}e^3 \right] + O(e^4), \\ -\frac{\pi}{2} < \arg e < 0 . \quad (90)$$

When $l_o > 0$, the path \mathcal{C}_{sd} of steepest descent starts at the origin of the complex plane with $\arg e = -\pi/4$. Unless R is very large compared to l_x and l_y , the terms of order e^4 of Eq. (90) are negligible in the semiclassical approximation. However, at grazing angles, $l_o/R \sim 0$, the leading dependence on the wave number comes from the term of order e^3 in Eq. (90). To obtain a semiclassical expansion that is uniformly valid in the whole classically shadowed region, one therefore has to retain all exponential terms with exponents that

are of cubic or lower order for small e . To semiclassical accuracy we have, using Eq. (90), σ given by Eq. (44), $B(0)$ by Eq. (79) and $f(e)$ by Eq. (78),

$$\begin{aligned} G_{\mathcal{C}_{sd}}(-R) &= \frac{i}{\pi\hbar} \int_{\mathcal{C}_{sd}} e \, de \, B(e) \frac{e^{i[(S(e)/\hbar)-f(e)]}}{1 - e^{-if(e)}} \\ &\sim \frac{B(0)}{2\pi i \hbar (kR)^{2/3}} P\left(\left(\frac{3}{4}\right)^{\frac{2}{3}} \sigma l_o\right) = \frac{(kR)^{1/3}}{4\pi i \sqrt{l_x l_y}} P\left(\left(\frac{3}{4}\right)^{\frac{2}{3}} \sigma l_o\right) \end{aligned} \quad (91)$$

(Note that this contribution to the Green function neatly separates into the product of free one-dimensional Green functions over distances l_x and l_y and a factor that depends on l_o and R .) For positive real values of z , the function $P(z)$ has the integral representation,

$$P(z) = i \sqrt[3]{18} \int_{\mathcal{C}_{sd}} \xi d\xi \frac{e^{-i(z\xi^2 + \xi^3)}}{1 + ie^{-i\xi^3}}. \quad (92)$$

$P(z)$ is an entire function that is defined in the whole complex plane by the convergent series (derived in Appendix C),

$$P(z) = i \left(\frac{2i}{3}\right)^{1/3} \sum_{n=1}^{\infty} \left(z e^{-5\pi i/6}\right)^{n-1} \frac{\Gamma(2n/3)}{\Gamma(n)} \text{Li}_{2n/3}(-i), \quad (93)$$

where

$$\text{Li}_\nu(\rho) = \sum_{n=1}^{\infty} \frac{\rho^n}{n^\nu} \quad (94)$$

is the poly-logarithm of order ν . Of particular interest are the asymptotic values of $P(z)$ for large and small z , corresponding to large and small values of kl_o :

$$\begin{aligned} P(0) &= i \left(\frac{2i}{3}\right)^{1/3} \Gamma(2/3) \text{Li}_{2/3}(-i) \approx 0.966 e^{0.00347\pi i} \\ P(z) &\sim \frac{3^{2/3} e^{-\frac{\pi i}{4}}}{2^{7/6} z} \approx \frac{0.927 e^{-\frac{\pi i}{4}}}{z}, \text{ for } |z| \sim \infty, \quad -\frac{\pi}{2} < \arg z < \frac{\pi}{2}. \end{aligned} \quad (95)$$

The asymptotic forms of Eq. (95) are most easily obtained from Eq. (92); see Appendix C.

To finally obtain $G_r(0, 0; \tau_c, R)$ we again analytically continue the expressions in Eqs. (91) and (85) to negative values of R in such a manner that G_r remains bounded for large values of l_o . We thus find that the semiclassical approximation to the Green function for the radial coordinate from a single extremal path whose end-point is in the shadow of a sphere of radius R is

$$G_r(0, 0; \tau_c, R) = \frac{ik}{4\pi \bar{\sigma} R} \left[\frac{P\left(\left(\frac{3}{4}\right)^{\frac{2}{3}} \bar{\sigma} l_o\right)}{2^{2/3} \bar{\sigma} \sqrt{l_x l_y}} + \sum_{n=0}^{\infty} D_n(\bar{\sigma} l_x) D_n(\bar{\sigma} l_y) e^{-i\bar{\sigma} l_o \bar{\epsilon}_n} \right] \quad (96)$$

The diffraction amplitudes $D_n(\xi)$ are defined by Eqs. (86) and (87), with $\bar{\epsilon}_n$ given by Eq. (83) and $\bar{\sigma}$ by Eq. (54). The function $P(z)$ for complex z is defined by the expansion Eq. (93).

4.4 The Penumbra near the Glancing Ray with $l_o = 0$

The correction from the contour C_{sd} in Eq. (96) is essential for describing the penumbra. We compare our result with the asymptotic form of the exact solution in the penumbra obtained in [5, 6]. In the penumbra $kl_o \ll kR$ and one can expand G_r in powers of kl_o . The leading term in this expansion of G_r is

$$G_r(0, 0; \tau_c, R)|_{l_o=0} = \frac{ik}{4\pi\bar{\sigma}R} \left[\frac{P(0)}{2^{2/3}\bar{\sigma}\sqrt{l_x l_y}} + \sum_{n=0}^{\infty} D_n(\bar{\sigma}l_x) D_n(\bar{\sigma}l_y) \right]. \quad (97)$$

The sum in Eq. (97) is exponentially damped and converges for any value of kR . Let $\xi = \bar{\sigma}l$, with $l = l_x$ or l_y ; $\bar{\sigma}$ is given by Eq. (54). For $\bar{\epsilon}_n \gg |\xi|^2$, we find on using Eq. (87) that

$$\bar{p}_n(\xi) \sim \bar{\epsilon}_n^{1/2} - \xi, \quad (98)$$

and therefore that

$$\frac{2}{3}\bar{p}_n^3(\xi) + \xi\bar{p}_n^2(\xi) \sim \frac{2}{3}\bar{\epsilon}_n^{3/2} - \xi\bar{\epsilon}_n. \quad (99)$$

Since $\text{Im}(\xi) < 0$, $D_n(\xi)$ defined by Eq. (86) therefore decays exponentially and the contribution to the sum in Eq. (97) from terms with $\bar{\epsilon}_n \gg |\xi|^2$ is negligible.

We now assume that $\bar{\epsilon}_n \ll |\xi|^2$. For $|\bar{\epsilon}_n/\xi^2| \ll 1$,

$$\bar{p}_n(\xi) \sim \bar{\epsilon}_n/(2\xi) + O(|\xi|^{-3}). \quad (100)$$

Since $|\xi| \propto (kR)^{1/3}$, we can simplify the sum in Eq. (97) in the asymptotic limit we are interested in. Retaining only leading terms in kR , the definition Eq. (86) of the diffraction amplitudes leads to the simplification

$$\begin{aligned} \Sigma_D &\equiv \sum_{n=0}^{\infty} D_n(\bar{\sigma}l_x) D_n(\bar{\sigma}l_y) \\ &\sim \frac{\pi}{\bar{\sigma}\sqrt{l_x l_y}} \sum_{n=0}^{\infty} (\bar{\epsilon}_n)^{-\frac{1}{2}} \exp \left[i \frac{\bar{\epsilon}_n^2}{4\bar{\sigma}} \frac{l_x + l_y}{l_x l_y} \right] \equiv \frac{\pi}{\bar{\sigma}\sqrt{l_x l_y}} \sum_{n=0}^{\infty} \Phi(n) \end{aligned} \quad (101)$$

The sum over n in Eq. (101) is effectively cut off when $\bar{\epsilon}_n^2$ becomes of order $1/\Lambda$ or larger, where

$$\Lambda = \frac{l_x + l_y}{|\bar{\sigma}|l_x l_y}. \quad (102)$$

Since for large values of ξ , $\bar{\epsilon}_n \sim 1/\Lambda \sim |\xi| \ll |\xi|^2$, the sum in Eq. (101) effectively never extends to values of n where the expansion of Eq. (100) is not justified.

We appeal to the Abel-Plana formula [22],

$$\sum_{n=0}^{\infty} \Phi(n) = \frac{\Phi(0)}{2} + \int_0^{\infty} dn \Phi(n) + i \int_0^{\infty} dz \frac{\Phi(iz) - \Phi(-iz)}{\exp(2\pi z) - 1}, \quad (103)$$

to evaluate the sum in Eq. (101) asymptotically. In the evaluation of the first and third terms of Eq. (103), we approximate the exponential factor in Eq. (101) by unity. We find, using Eq. (83) that,

$$\frac{\Phi(0)}{2} = \frac{1}{2\sqrt{\epsilon_0}} = \left(\frac{1}{9\pi}\right)^{1/3} + O(\Lambda), \quad (104)$$

to leading order in Λ . To the same accuracy, the third term of Eq. (103) becomes,

$$-2 \left(\frac{2}{3\pi}\right)^{\frac{1}{3}} \int_0^\infty dz \frac{\text{Im}[(iz + \frac{3}{4})^{-\frac{1}{3}}]}{\exp(2\pi z) - 1} + O(\Lambda). \quad (105)$$

To evaluate the integral over n of the second term in Eq. (103), we change the integration variable from n to $\bar{\epsilon}_n$, using Eq. (83). We then find that

$$\int_0^\infty dn \Phi(n) = \int_{\frac{(9\pi)^{2/3}}{4}}^\infty \frac{d\epsilon}{\pi} \exp\left[i\frac{\epsilon^2}{4\bar{\sigma}} \frac{l_x + l_y}{l_x l_y}\right] \sim \sqrt{\frac{i\bar{\sigma} l_x l_y}{\pi(l_x + l_y)}} - \frac{(9\pi)^{2/3}}{4\pi} + O(\Lambda). \quad (106)$$

Collecting the results and using the them in Eq. (97), the Green function at the grazing angle is found to have the asymptotic form,

$$G_r(0, 0; \tau_c, R)|_{l_o=0} = \frac{1}{2} \sqrt{\frac{k}{2\pi i(l_x + l_y)}} + K \frac{(kR)^{\frac{1}{3}} e^{\pi i/3}}{4\pi i \sqrt{l_x l_y}} + O\left(\frac{R(l_x + l_y)}{(l_x l_y)^{\frac{3}{2}}}\right). \quad (107)$$

For large values of kR , the Green function at the grazing angle is just half the direct term, with an additional contribution[6] proportional to $(kR)^{\frac{1}{3}}$. The proportionality constant K of the latter is

$$\begin{aligned} K &= P(0) + \frac{\pi}{(9\pi/4)^{1/3}} - \left(\frac{9\pi}{4}\right)^{\frac{2}{3}} - 2 \left(\frac{\pi^2}{3}\right)^{\frac{1}{3}} \int_0^\infty dz \frac{2\text{Im}(iz + \frac{3}{4})^{-\frac{1}{3}}}{\exp(2\pi z) - 1} \\ &= P(0) - 2\text{Re}P(0) = -P^*(0) \approx -0.966e^{-0.00347\pi i}. \end{aligned} \quad (108)$$

(-)Re K differs from the coefficient $c \approx 0.996$ for the glancing contribution to the Green function of Rubinow and Wu [6] by about 3%; we find $\text{Im}P(0) = -\text{Im}K =$ to be very small, while in[6] it is found to be zero. The small discrepancy arises because the integral over a ratio of Airy functions that defines c is evaluated numerically in [6], rather than in saddle point approximation. Our approach is perhaps slightly more consistent – that does not imply that it is more accurate – and in any event, the difference is quite small.

It perhaps is of some interest that the correction of order $(kR)^{1/3}$ for the glancing ray does not appear in $\mathcal{G}_r(0, 0; \tau_c)$. Eqs. (40) and (37) imply that

$$\begin{aligned} \mathcal{G}_r(0, 0; \tau_c)|_{\tau_o=0} &= \frac{k}{2\pi i} \int_0^\infty \frac{da}{\sqrt{l_x}} \int_0^\infty \frac{db}{\sqrt{l_y}} \delta(a - b) \exp\left(\frac{ika^2}{2l_x} + \frac{ikb^2}{2l_y}\right) \\ &= \frac{1}{2} \sqrt{\frac{k}{2\pi i(l_x + l_y)}}, \end{aligned} \quad (109)$$

without further corrections. Physically, this discrepancy can be traced to the assumed decomposition of the radial Green function in Eq. (37). The lower bound of the integral over the radial coordinates in Eq. (37) can be set to zero only for $k = \infty$. For large but finite wave number k , the correction of order $(kR)^{1/3}$ is reproduced by assuming that the fluctuations effectively penetrate the obstacle a small distance $d_o(k, R)$. Replacing the lower bound of the radial integrals in Eq. (109) by $-d_o(k, R)$, one finds,

$$\begin{aligned} \mathcal{G}_r(0, 0; \tau_c)|_{\tau_o=0} &= \frac{k}{2\pi i \sqrt{l_x l_y}} \int_{-d_o}^{\infty} da \exp\left(\frac{ika^2(l_x + l_y)}{2l_x l_y}\right) \\ &\sim \frac{1}{2} \sqrt{\frac{k}{2\pi i(l_x + l_y)}} - \frac{kd_o}{2\pi i \sqrt{l_x l_y}} + O(d_o^3). \end{aligned} \quad (110)$$

Comparison of Eq. (110) with Eq. (107) leads to

$$d_o(R, k) \sim -K \frac{(kR)^{1/3} e^{\pi i/3}}{2k} \quad (111)$$

for $d_o(k, R)$. The effective depth of penetration thus vanishes rather slowly, as $k^{-2/3}$. The phase $e^{\pi i/3}$ in the expression Eq. (111) for d_o has its origin in the analytic continuation of R to $-R$, and the proportionality constant K is very close to -1 .

The true semiclassical Green function G_r does not in general separate into free- and creeping- Green functions, and approximately reproduces the subleading asymptotic contributions as well (to within about 3%).

5 Discussion, Generalization and Conclusion

The semiclassical description of diffraction is closely associated with extremal classical paths that satisfy Fermat's principle but are *not* stationary. Such paths arise due to the non-holonomic constraints imposed by "obstacles". The associated Lagrangian is given in Eq. (23). It depends on the transverse deviations $\underline{x}_r(t), \underline{x}_\perp(t)$ from the classical path and describes the two-dimensional motion of a non-relativistic particle of mass $m_E = E/v^2(E)$ under the influence of a spatially constant but in general time-dependent, force $m_E g(t)$. The acceleration $g(t)$ is inversely proportional to the curvature of the classical path and vanishes for time intervals in which the classical path γ_c is not constrained by an obstacle. On "creeping" sections of the classical trajectory, fluctuations are in addition restricted to the half-space exterior to the obstacle.

Depending on the sign of the curvature, $g(t)$ is either directed toward or away from the obstacle's surface – corresponding to the presence of (a generally time dependent) "floor" or "ceiling" in an analogous 1-dimensional gravitational-like problem. Motion in the presence of a "floor" is relevant for "whispering-galleries", for example, whereas the presence of a "ceiling" corresponds to diffraction into the classical shadow of an obstacle.

Diffraction is semiclassically described by the amplitude that the particle moves from the ceiling to the ceiling in a fixed time interval with acceleration $g(t)$. This motion is classically forbidden. To calculate the amplitude semiclassically, we relate it to the one for motion from the "floor" to the "floor" with acceleration $g(t)$. The latter problem, that of a "whispering gallery", admits classical solutions. The amplitudes of the two problems are related by analytic continuation in the phase ϕ of the curvature $R(t) \rightarrow |R(t)|e^{i\phi}$ of the classical path.

The existence of a caustic, the "floor", that is approached by an infinite number of classical paths poses an additional problem in the semiclassical description. For any fixed value of k , there are distinct classical paths whose actions differ by much less than \hbar . The fluctuations about different classical paths therefore cannot be separated and tend to interfere with each other. Attempting to evaluate the path integral asymptotically by summing the asymptotic contributions of every individual classical path becomes highly inaccurate.

The problem was solved for the special case of a classical ray that partially creeps along the surface of a sphere; the asymptotic analysis of the same problem was also at the heart of the original geometrical interpretation of diffraction[1, 2]. The curvature of this trajectory is piecewise constant and corresponds to an acceleration $g(t)$ that is piecewise constant in time. A path with n bounces in total time τ_c is stationary with respect to a variation of the (conserved) "energy", e_n , of the particle in the region of constant acceleration. One thus can express the asymptotic contribution from a classical path to given n as the result of an integral over the "energy" e that is evaluated semiclassically at the saddle point $e = e_n$. This manipulation is consistent with the semiclassical approximation and allows one to sum over n for a given "energy" e *before* evaluating the remaining integral over e asymptotically.

In the case of a sphere, the exact expression for the Green function of a massless particle is known and has been evaluated asymptotically in the umbra[1] of the sphere as well as in its penumbra[5, 6]. Quite different asymptotic forms were found for the two cases. The procedure outlined above and described in more detail in section 3 gives a uniform asymptotic expansion that is valid in both regions: the exponentially decaying terms arise from pole contributions to the final integral over e , whereas power corrections (previously obtained separately for the penumbra[6]) turn out to be associated with an end-point contribution to the integral at $e = 0$.

The basic analysis through section 4 is applicable to a much more general case, but the derivation of a relatively simple explicit form of the asymptotic Green function, Eq. (96), was obtained only for the spherical case. The procedure can in principle be modified to include cases where the curvature $R(t)$ is *not* piecewise constant. Because the acceleration is not constant, the energy e_n in this case is not conserved on the creeping segment. One nevertheless may, for instance, express the action $S_n(h_n)$ of a classical path with n bounces in terms of, say, the maximal "height" h_n of the classical trajectory. It is not difficult to verify that h_n is a stationary point of $S_n(h)$ if one allows this height to vary while keeping fixed the endpoints and number of "bounces" n . One can

then proceed as in section 4 and express the semiclassical approximation to the Green function as an integral over h and first sum over the number of bounces n before evaluating the integral over h asymptotically. However, unlike the case considered in section 4, the summation over n generally cannot be performed in closed form if the acceleration is not piecewise constant. One nevertheless may sometimes be able to pick out the smallest values of h for which the sum over n becomes singular and thus (numerically) obtain the leading asymptotic approximation in the general case.

With a view to applying the method to electromagnetic problems with ideal conductors, we considered only Dirichlet boundary conditions, with a change in the phase by (-1) at each reflection. Semiclassically, other idealized boundary conditions change the phase by a different value. Furthermore, if absorption cannot be neglected, the modulus of the reflection coefficient is less than unity. Although the physical effect of such changes can be dramatic, since the poles are moved, it is a great virtue of the semiclassical approximation that neither changes in the boundary conditions nor the inclusion of absorption alter the procedure in any fundamental way.

We briefly comment now on two related papers. Our approach is similar in spirit to the one of V.N. Buslaev[23]. Buslaev writes the Green function G as a "continuum integral" product of Green functions for infinitesimal time intervals and uses the saddle point method to obtain the asymptotic form of each factor. We do not explicitly use the product form and treat the problem by expansion about the classical paths of extremal, but finite, length. Our approach appears to be simpler and reduces the diffraction problem to the propagation of a particle in a two-dimensional space under the influence of a gravitational-like force. However, Buslaev considers a mathematically more general problem than we do, that is asymptotic solutions to general parabolic equations. He also does not restrict the dimensionality of space to three. Furthermore, our treatment of the boundary conditions is very different from that of Budaev. McLaughlin and Keller[24] note that Buslaev's result agrees with Keller's geometrical theory of diffraction for the field of a surface diffracted ray. An interesting alternative to these methods may be the solution of the wave equation by analytic continuation of a random walk proposed in ref.[25].

Acknowledgements: We thank J.B. Keller for bringing references[23] and[25] to our attention and for a number of useful comments. This work was supported by the National Science Foundation with Grant PHY-0070525. M.S. greatly enjoyed the hospitality of New York University.

A The Proportionality Factor

To derive the relation of Eq. (28) between the semiclassical energy Green function $G(\mathbf{X}, \mathbf{Y}; E)$ and the Green functions \mathcal{G}_{γ_c} defined in Eq. (27) that describes transverse deviations from a classical path γ_c , consider first the general case of a medium with a smooth, everywhere differentiable index of refraction $n(\mathbf{X}, E)$. In this case classical trajectories γ_c from \mathbf{X} to \mathbf{Y} are stationary points of the

action and the usual semiclassical formalism applies. In particular, the semiclassical energy Greenfunction is given[17] by,

$$G(\mathbf{X}, \mathbf{Y}; E) = \sum_{\gamma_c} \frac{1}{2\pi\hbar^2} \sqrt{D_{\gamma_c}} \exp\left(\frac{i}{\hbar} S(\gamma_c, E)\right). \quad (112)$$

For a given classical path γ_c , D_{γ_c} is the determinant of a 4×4 matrix,

$$D_{\gamma_c} = \det \left(\begin{array}{c|c} \frac{\partial^2 S(\gamma_c, E)}{\partial \mathbf{X} \partial \mathbf{Y}} & \frac{\partial^2 S(\gamma_c, E)}{\partial \mathbf{X} \partial E} \\ \hline \frac{\partial^2 S(\gamma_c, E)}{\partial \mathbf{Y} \partial E} & \frac{\partial^2 S(\gamma_c, E)}{\partial E^2} \end{array} \right), \quad (113)$$

with elements that are 3×3 , 3×1 , 1×3 and 1×1 matrices. The form of D_{γ_c} can be simplified by choosing a local coordinate system in the neighborhood of the trajectory γ_c from \mathbf{X} to \mathbf{Y} : the coordinate axis for x_{\parallel} runs along the particular trajectory and the remaining coordinates $\vec{x} = (x_r, x_{\perp})$ are transverse to the trajectory. Since $1/v_g$ at the endpoint of a trajectory is just the change in the total time Eq. (6) associated with an infinitesimal displacement of the endpoint in a direction tangent to the trajectory, two of the second variations of the action in Eq. (113) are given by the group velocities at the endpoints, namely,

$$\begin{aligned} v_g^{-1}(\mathbf{X}, E) &= -\frac{\partial \mathcal{T}}{\partial x_{\parallel}} = -\frac{\partial^2 S(\gamma_c, E)}{\partial x_{\parallel} \partial E} \\ v_g^{-1}(\mathbf{Y}, E) &= \frac{\partial \mathcal{T}}{\partial y_{\parallel}} = \frac{\partial^2 S(\gamma_c, E)}{\partial y_{\parallel} \partial E} \end{aligned} \quad (114)$$

In this coordinate system, D_{γ_c} becomes[17]

$$D_{\gamma_c} = \frac{1}{v_g(\mathbf{X}, E)v_g(\mathbf{Y}, E)} \det \left(\frac{-\partial^2 S(\gamma_c, E)}{\partial \vec{x} \partial \vec{y}} \right), \quad (115)$$

proportional to the determinant of a 2×2 matrix. Crucial in deriving Eq. (28) is the observation that the matrix of second derivatives of S with respect to *transverse* deviations from the classical path γ_c at the endpoints can also be obtained by expanding S to quadratic order in the transverse deviations of the path γ from the classical path γ_c . We thus have that

$$\left(\frac{-\partial^2 S(\gamma_c, E)}{\partial \vec{x} \partial \vec{y}} \right) = \left(\frac{-\partial^2 S_{\gamma_c}^{sc}(\vec{a} = \vec{b} = 0; \tau(\gamma_c, E))}{\partial \vec{a} \partial \vec{b}} \right) \quad (116)$$

On the other hand, if $v(\mathbf{X}, E)$ is a smooth function of the coordinate, the classical trajectory γ_c is stationary and S^{sc} is quadratic in the fluctuations. In this case, the semiclassical approximation to $\mathcal{G}_{\gamma_c}(\vec{a}, \vec{b}; \tau)$ is exact. The solution to

the equation of motion for a quadratic action S^{sc} is unique and there is only one classical trajectory $\tilde{\gamma}_c$ from \vec{a} to \vec{b} in time τ that contributes to the two-dimensional Greenfunction $\mathcal{G}_{\gamma_c}(\vec{a}, \vec{b}; \tau)$. Van Vleck's formula in two-dimensional space[21] then gives

$$\mathcal{G}_{\gamma_c}(\vec{a}, \vec{b}; \tau) = \frac{1}{2\pi i \hbar} \sqrt{\det \left(\frac{-\partial^2 S_{\gamma_c}^{sc}(\vec{a}, \vec{b}; \tau)}{\partial \vec{a} \partial \vec{b}} \right)} \exp \left\{ \frac{i}{\hbar} S_{\gamma_c}^{sc}(\vec{a}, \vec{b}; \tau) \right\} . \quad (117)$$

Note that the only classical trajectory from $\vec{a} = 0$ to $\vec{b} = 0$ in time $\tau(\gamma_c, E)$ is the trivial one with vanishing transverse deviation everywhere and that therefore

$$S(\gamma_c, E) = S_{\gamma_c}^{sc}(\vec{a} = \vec{b} = 0; \tau(\gamma_c, E)) . \quad (118)$$

Comparing Eq. (117) with Eq. (112) for $\tau = \tau(\gamma_c, E)$ and $\vec{a} = \vec{b} = 0$ and using Eqs. (118), (116) and (115), one arrives at the relation Eq. (28).

Strictly speaking the validity of Eq. (28) has only been shown for a smooth, everywhere differentiable phase velocity $v(\mathbf{X}, E)$. In this case the classical trajectories γ_c are stationary points of the action and the semiclassical expressions we employed are valid. We argue that Eq. (28) also holds when $v(\mathbf{X}, E)$ is a step function that vanishes within \mathcal{V} , because Eq. (28) does not explicitly depend on the spatial dependence of $v(\mathbf{X}, E)$ and involves only the group velocities at the endpoints of the classical trajectories. Eq. (28) does not depend on the nature of the obstacle and the discontinuous spatial dependence of the phase velocity of interest can be considered as a limiting case. One similarly can argue that because Eq. (28) holds for endpoints \mathbf{X} and \mathbf{Y} connected by classical trajectories that do not touch the obstacle, the relation should by continuity remain valid when one of the endpoints lies in the classical shadow region of the other.

B Proof that $\mathcal{D}_n(\xi) \rightarrow D_n(\xi)$ for $n \rightarrow \infty$

It is instructive to see that the diffraction amplitudes defined in Eqs. (57) and (86) coincide in the limit of large n for any fixed real value of ξ . For large $n \sim \infty$ the zero's of the Airy function ϵ_n approach $\bar{\epsilon}_n$ defined by Eq. (83); in particular, ϵ_n becomes arbitrarily large for $n \rightarrow \infty$.

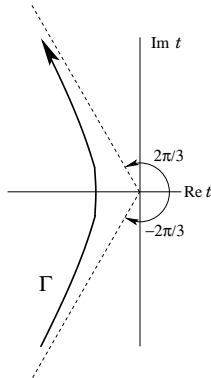


Fig. 5: The contour Γ in the representation for the Airy-function $\text{Ai}(z)$ of Eq. (119). For large values of $|t|$, Γ approaches the asymptotes with $\arg t = \pm 2\pi/3$ shown as dashed lines.

The Airy function can be represented by the contour integral[18]

$$\text{Ai}(z) = \frac{1}{2\pi i} \int_{\Gamma} dt e^{tz - t^3/3} , \quad (119)$$

where the contour Γ is sketched in Fig. 5. The expression for $\mathcal{D}_n(\xi)$ of Eq. (57) then becomes

$$\mathcal{D}_n(\xi) = \frac{1}{2\pi i |\text{Ai}'(-\epsilon_n)|} \int_0^{\infty} d\rho \int_{\Gamma} dt e^{i \frac{\rho^2}{4} - \frac{\rho^3}{3} + t\rho\sqrt{\xi - t\epsilon_n}} . \quad (120)$$

For large values of ϵ_n the saddle-point approximation to the integral of Eq. (120) is accurate. The two saddle points of the integrand are located at

$$\bar{\rho}_n^{\pm} = 2\sqrt{\xi} \bar{p}_n^{\pm}(\xi) , \quad \bar{t}_n^{\pm} = -i\bar{p}_n^{\pm}(\xi) , \quad (121)$$

with

$$\bar{p}_n^{\pm}(\xi) = \pm \sqrt{\epsilon_n + \xi^2} - \xi . \quad (122)$$

For large values of n , $\bar{\rho}_n^-$ is negative and does not contribute to the saddle point approximation of the integral. The path of integration can, however, be deformed to pass over the other stationary point at $(\bar{\rho}_n^+, \bar{t}_n^+)$. The integral of Eq. (120) in saddle point approximation thus becomes,

$$\mathcal{D}_n(\xi) \sim \frac{1}{|\text{Ai}'(-\epsilon_n)|(\epsilon_n + \xi^2)^{1/4}} \exp i \left[\frac{2}{3} (\bar{p}_n^+(\xi))^3 + \xi (\bar{p}_n^+(\xi))^2 \right] . \quad (123)$$

One finally arrives at the expression of Eq. (86) for $D_n(\xi)$ by using the asymptotic formula for the Airy function. Eq. (47) implies that for large n ,

$$\epsilon_n \sim \bar{\epsilon}_n , \quad \bar{p}_n^+(\xi) \sim \bar{p}_n(\xi) \quad \text{and} \quad |\text{Ai}'(-\epsilon_n)| \sim \bar{\epsilon}_n^{1/4} / \sqrt{\pi} , \quad (124)$$

where $\bar{\epsilon}_n$ and $\bar{p}_n(\xi)$ are defined in Eqs. (83) and (87), respectively. Although the amplitudes $\mathcal{D}_n(\xi)$ and $D_n(\xi)$ coincide for large values of n , this does not mean that the contribution from the poles of Eq. (85), by itself, gives the correct asymptotic expansion of the Green function. The asymptotic expansion of the Green function is in fact dominated by low- n terms, and we indeed obtained asymptotic corrections to the pole contributions in the semiclassical approximation.

C Asymptotics of $P(z)$

The function $P(z)$ defined by Eq. (92) may be written as a McLaurin series,

$$P(z) = \sum_{n=1}^{\infty} \frac{(-iz)^{n-1}}{\Gamma(n)} P_n, \quad (125)$$

with coefficients P_n given by

$$P_n = \sqrt[3]{18} \int_{\mathcal{C}_{sd}} \xi^{2n-1} d\xi \frac{ie^{-i\xi^3}}{1+ie^{-i\xi^3}} = -\sqrt[3]{18} \sum_{k=1}^{\infty} (-i)^k \int_{\mathcal{C}_{sd}} \xi^{2n-1} d\xi e^{-ik\xi^3}. \quad (126)$$

For given k , the integral for the contour \mathcal{C}_{sd} of Fig. 4 can be performed by making the substitution

$$\xi = \sqrt[3]{\rho/k} e^{-i\pi/6}, \quad (127)$$

where ρ is real, and using the definition (94). We then have

$$\begin{aligned} P_n &= -\frac{\sqrt[3]{18}}{3} e^{-i\pi n/3} \Gamma(2n/3) \sum_{k=1}^{\infty} \frac{(-i)^k}{k^{2n/3}} \\ &= i(2i/3)^{1/3} e^{-\frac{i\pi(n-1)}{3}} \Gamma(2n/3) \text{Li}_{2n/3}(-i). \end{aligned} \quad (128)$$

Eqs. (125) and (128) give the convergent series of Eq. (93). Note that the series in Eq. (93) uniquely defines $P(z)$ in the whole complex plane but for $|z| \gg 1$, the accurate evaluation of $P(z)$ requires a sizable number of terms and is numerically not very efficient.

For $|z| \gg 1$, terms of order ξ^3 in the exponent may be ignored to leading order of the steepest descent method and the integral of Eq. (92) approaches the asymptotic form in Eq. (95),

$$P(z \gg 1) \sim i\sqrt[3]{18} \int_{\mathcal{C}_{sd}} \xi d\xi \frac{e^{-iz\xi^2}}{1+i} = \frac{3^{2/3}}{2^{7/6}z} e^{-i\pi/4}. \quad (129)$$

For real x , $P(x)$ is a rather slowly changing function of x that smoothly interpolates between $P(0)$ and $P(x \gg 1)$. For real positive x , $P(x)$ is numerically approximated by the rational function

$$P(x) \approx \frac{0.7(1-i)}{0.7(1-i) + x} \quad (130)$$

to within about 10%.

References

- [1] J.B. Keller, J. Opt. Soc. Amer. **52**, 116 (1962), and references therein.
- [2] A wealth of material on the geometrical approach to diffraction is in J.B. Keller and R.M. Lewis, *Asymptotic Theory of Wave Propagation and Diffraction*, unpublished book manuscript in 2 Volumes, (Courant Institute, New York University, 1970).
- [3] Early applications of the geometrical theory of diffraction are in J.B. Keller, J. Appl. Phys. **30**, 1452 (1952); B.R. Levy and J. Keller, Commun. Pure Appl. Math. **12**, 159 (1959); D. Magiros and J.B. Keller, Commun. Pure Appl. Math. **14**, 457 (1961); K.O. Friedrichs and J.B. Keller, J. Appl. Phys. **26**, 961 (1955).
- [4] G. Vattay, A. Wirzba and P.E. Rosenqvist, Phys. Rev. Lett. **73**, 2304 (1994).
- [5] R.N. Buchal and J.B. Keller, Commun. Pure Appl. Math. **13**, 85 (1960); H. Primack, H. Schranz, U. Smilansky and I. Ussishkin, Phys. Rev. Lett. **76**, 1615 (1996).
- [6] S.I. Rubinow and T.T. Wu, J. Appl. Phys. **27**, 1032 (1956); H.M. Nussenzweig, Ann. Phys. **34**, 23 (1965); H. Primack, H. Schranz, U. Smilansky and I. Ussishkin, J. Phys. A:Math. Gen. **30**, 6693 (1997).
- [7] R.P. Feynman, Phys. Rev. **76**, 749 (1949); *ibid*, 769 (1949); See also R.P. Feynman and A.R. Hibbs, *Quantum Mechanics and Path Integrals*, (McGraw-Hill, New York, 1965), Chap. 2.
- [8] M.C. Gutzwiller, *Chaos in classical and quantum mechanics* (Springer Verlag, New York, 1990) and references therein.
- [9] M. Schaden and L. Spruch, Phys. Rev. **A58**, 935 (1998).
- [10] B.V. Derjaguin, I.I. Abrikosova and E.M. Lifshits, Quarterly Rev. **10**, 295 (1968). See also P.W. Milloni, *The Quantum Vacuum* (Academic Press, New York, 1994), p.272.
- [11] V.M. Mostepanenko and V.N. Trunov, *The Casimir Effect and its Applications* (Clarendon Press, Oxford, 1997).
- [12] H.G.B. Casimir and D. Polder, Phys. Rev. **73**, 360 (1948).
- [13] L.E. Reichl, *The Transition to Chaos* (Springer-Verlag, New York, 1992).
- [14] For the literature on caustic surfaces see, for example, Yu.A. Kravtsov and Yu.I. Orlov, *Caustics, Catastrophes and Wave Fields* – 2nd ed., (Springer-Verlag, Berlin, 1999); J.F. Nye, *Natural Focusing and Fine Structure of Light* (IOP, Bristol, 1999); C. DeWitt-Morette and P. Cartier in *Functional Integration, Basics and Applications*, eds. C. DeWitt-Morette, P. Cartier and A. Folacci, (Plenum, New York 1997) Nato ASI Series **B361** 97.

- [15] Motion on a helix with constant speed $v = \sqrt{v_z^2 + (R_{\text{cyl}}\omega)^2}$ can be parameterized by $\mathbf{X}_{\text{helix}}(t) = (R_{\text{cyl}} \cos(\omega t), R_{\text{cyl}} \sin(\omega t), v_z t)$, where ω is the constant clockwise angular velocity around the cylinder of radius R_{cyl} and v_z is the velocity component parallel to the axis of the helix. (R_{cyl} is the curvature of the helical path only if $v_z = 0$.) Using Eq. (8) to obtain the corresponding local basis vectors and evaluating Eq. (15), one finds that $\alpha = -\omega v_z/v$ in this case.
- [16] J.J. Sakurai, *Quantum Mechanics* Rev. ed. (Addison-Wesley, New York, 1994) p.108.
- [17] Ref.[8], Sec. 2.4 and Ref.[13], Chap. 8.
- [18] *Handbook of Mathematical Functions* eds. M. Abramowitz and I.A. Stegun (National Bureau of Standards, Washington, 1964), p.446ff.
- [19] The whole semiclassical approximation is only of pedagogical value in the case of a sphere, since the exact spectral representation of the Green function of a massless particle excluded from a spherical region is known.
- [20] A "bounce" here is analogous to an "instanton" solution in Quantum Field Theory in the sense that it too is a time-dependent and topologically stable solution of the classical equation of motion.
- [21] See Ref.[8], Sec. 12.5.
- [22] See Ref.[11], Sec. 2.2.
- [23] V.N. Buslaev, *Topics in Math. Phys.* **2**, (1968) 67.
- [24] D. McLaughlin and J.B. Keller, *Am. Math. Monthly* **82** (1975),451.
- [25] B.V. Budaev, D.B.Bogy, *Random walk approach to wave propagation in wedges and cones*, University of California preprint Nov.12 (2002).